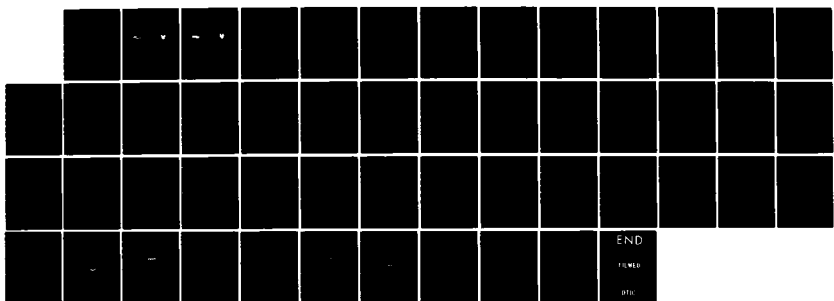


AD-A150 478 LASER DIAGNOSTIC ANALYSES OF SOOTING FLAMES(U) UNITED 1/1
TECHNOLOGIES RESEARCH CENTER EAST HARTFORD CT
G M DOBBS ET AL. 29 NOV 84 UTRC/R84-955388-F

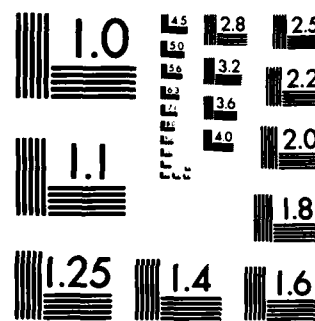
UNCLASSIFIED N00014-81-C-0046

F/G 21/2

NL



END
REVIEWED
ptm



MICROCOPY RESOLUTION TEST CHART
NATIONAL BUREAU OF STANDARDS 1963-A

**Final Report
Contract N00014-81-C-0046; NR 094-411**

LASER DIAGNOSTIC ANALYSES OF SOOTING FLAMES

AD-A150 478



UNITED TECHNOLOGIES RESEARCH CENTER
Silver Lane
E. Hartford, CT 06108



**PRINCETON UNIVERSITY
Department of Mechanical
and Aerospace Engineering
Princeton, N.J. 08544**

29 November 1984

Final Report for Period 1 October 1980-
30 September 1984

卷之三

Approved for public release; distribution unlimited. Reproduction in whole or in part is permitted for any purpose of the United States Government.

**Prepared for
OFFICE OF NAVAL RESEARCH
800N. Quincy ST
Arlington, VA 22217**

85 02 11 110

**Final Report
Contract N00014-81-C-0046: NR 094-411**

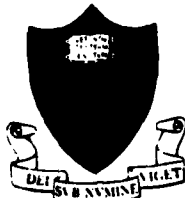
LASER DIAGNOSTIC ANALYSES OF SOOTING FLAMES

**Gregory M. Dobbs
Alan C. Eckbreth
Laurence R. Boedeker**



UNITED TECHNOLOGIES RESEARCH CENTER
Silver Lane
E. Hartford, CT 06108

**Irvin Glassman
Allesandro Gomez**



PRINCETON UNIVERSITY
Department of Mechanical
and Aerospace Engineering
Princeton, N.J. 08544

29 November 1984

Final Report for Period 1 October 1980- 30 September 1984

Approved for public release; distribution unlimited. Reproduction in whole or in part is permitted for any purpose of the United States Government.

**Prepared for
OFFICE OF NAVAL RESEARCH
800N. Quincy ST
Arlington, VA 22217**

Accession For
NTIS GRA&I
"TIC TAB
Unpublished
Classification



UNCLASSIFIED

SECURITY CLASSIFICATION OF THIS PAGE

REPORT DOCUMENTATION PAGE

1a. REPORT SECURITY CLASSIFICATION Unclassified		1b. RESTRICTIVE MARKINGS	
2a. SECURITY CLASSIFICATION AUTHORITY		3. DISTRIBUTION/AVAILABILITY OF REPORT Unlimited	
2b. DECLASSIFICATION/DOWNGRADING SCHEDULE			
4. PERFORMING ORGANIZATION REPORT NUMBER(S) R84-955388-F		5. MONITORING ORGANIZATION REPORT NUMBER(S)	
6a. NAME OF PERFORMING ORGANIZATION United Technologies Corp. Research Center	6b. OFFICE SYMBOL (if applicable)	7a. NAME OF MONITORING ORGANIZATION Office of Naval Research	
6c. ADDRESS (City, State and ZIP Code) Silver Lane East Hartford, CT 06108		7b. ADDRESS (City, State and ZIP Code) 800 N. Quincy Street Arlington, VA 22217	
8a. NAME OF FUNDING/SPONSORING ORGANIZATION Same as Block 7a.	8b. OFFICE SYMBOL (if applicable)	9. PROCUREMENT INSTRUMENT IDENTIFICATION NUMBER N0014-81-C-0046 NR094-411	
10. SOURCE OF FUNDING NOS.		PROGRAM ELEMENT NO. PROJECT NO. TASK NO. WORK UNIT NO.	
11. TITLE (Include Security Classification) Laser Diagnostic Analyses of Sooting Flames (U)			
12. PERSONAL AUTHOR(S) Gregory M. Dobbs, Alan C. Eckbreth, Laurence R. Boedeker, Irvin Glassman, and Allesandro Gomez		13. TYPE OF REPORT Final Report	
13b. TIME COVERED FROM 10/1/80 TO 9/30/84		14. DATE OF REPORT (Yr., Mo., Day) 84,11,29	15. PAGE COUNT 44
16. SUPPLEMENTARY NOTATION			
17. COSATI CODES		18. SUBJECT TERMS (Continue on reverse if necessary and identify by block number) Soot Formation, Diffusion Flames, Flame Structure, Temperatures in Diffusion Flames, CARS Temperature Measurement	
19. ABSTRACT (Continue on reverse if necessary and identify by block number) Temperature distributions and soot particle size distributions have been measured in axisymmetric, laminar, diffusion flames in order to provide the basis for modelling the influence of fuel structure and temperature on soot formation. This document is the final report and management summary for the joint activities of UTRC and Princeton University. Coherent anti-Stokes Raman spectroscopy (CARS) was used for non-intrusive determination of temperature. Soot particle size and number densities were determined by Mie scattering. The experimental results were then applied to current models of soot formation in an effort to determine the physical and chemical basis for fuel structure and temperature effects on soot formation in diffusion flames. In the course of this first application of CARS and Mie diagnostics to diffusion flames, a large number of questions was raised in regard to the structure of particulate-laden diffusion flames. Measured distributions were compared with a numerical flame-sheet model. <i>Original or furnished by [unclear]</i>			
20. DISTRIBUTION/AVAILABILITY OF ABSTRACT UNCLASSIFIED/UNLIMITED <input checked="" type="checkbox"/> SAME AS RPT. <input type="checkbox"/> DTIC USERS <input type="checkbox"/>		21. ABSTRACT SECURITY CLASSIFICATION Unclassified	
22a. NAME OF RESPONSIBLE INDIVIDUAL		22b. TELEPHONE NUMBER (Include Area Code)	22c. OFFICE SYMBOL

Laser Diagnostic Analyses of Sooting Flames

TABLE OF CONTENTS

	<u>Page</u>
SUMMARY	1
INTRODUCTION	2
Background and Importance of Results	2
Summary of Major Results	3
Organization of Report	5
APPARATUS DEVELOPMENT	6
CARS MEASUREMENTS	6
CARS Data Acquisition	7
CARS Temperature Calculations	10
Summary	10
PARTICLE-SIZING MEASUREMENTS	11
NUMERICAL MODELLING	14
VELOCITY DIAGNOSTICS	15
DATA BASE	17
CARS Measurements	17
Mie Measurements	18
RESULTS AND DISCUSSION	19
Soot Formation	19
Flame Structure	20
Areas for Future Work	21
REFERENCES	22
APPENDIX A	24

FIGURES

	<u>Page</u>
Figure A-1. Schematic of diffusion flame apparatus	31
Figure A-2. Optical configuration.	32
Figure A-3. Particle diameter as a function of radius and nondimensionalized height for the lower region of the butene flames.	33
Figure A-4. Particle diameter as a function of radius and nondimensionalized height for the upper region of butene flames	34
Figure A-5. Particle diameter as a function of radius and nondimensionalized height for the lower region of the undiluted butene flame and the diluted benzene flame	35
Figure A-6. Particle diameter as a function of radius and nondimensionalized height for the upper region of the undiluted butene flame and the diluted benzene flame	36
Figure A-7. Volume fraction or function of radius and nondimensionalized height for the lower region of the butene flames.	37
Figure A-8. Volume fraction as a function of radius and nondimensionalized height for the lower region of the butene flames.	38
Figure A-9. Volume fraction as a function of radius and nondimensionalized height for the lower region of the undiluted butene flame and the diluted benzene flame	39
Figure A-10. Volume fraction as a function of radius and nondimensionalized height for the upper region of the undiluted butene flame and the diluted benzene flame	40
Figure A-11. Number density as a function of radius and nondimensionalized height for the lower region of the butene flames.	41

SUMMARY

This document is the final report and management summary for Contract N00014-81-C-0046; NR 094-411, Laser Diagnostic Analyses of Sooting Flames, sponsored by the Office of Naval Research and conducted jointly by United Technologies Research Center and Princeton University. This research program consisted of non-intrusive determination of temperatures and soot particle size and number densities within sooting diffusion flames using coherent anti-Stokes Raman spectroscopy (CARS) and Mie scattering, respectively. The determined properties were then applied to current models of soot formation in an effort to determine the physical and chemical basis for fuel structure and temperature effects on soot formation in diffusion flames. In the course of this first application of CARS and Mie diagnostics to diffusion flames, a large number of questions was raised in regard to the structure of particulate-laden diffusion flames.

INTRODUCTION

Background and Importance of Results

Major changes in U. S. refinery operations have appreciably affected the character of the residual fuel components and thus the fuels currently being marketed for jet engine and diesel use. A consequence of this change is that jet and diesel engines currently produce extensive amounts of soot which have led to serious problems with respect to engine durability and emission characteristics. From a military point of view, increased soot in jet engine combustor cans decreases combustor lifetime substantially due to an increase in radiant heat transfer from the particle laden combustion gases to the can liners. Even more significant is the readily visible signature now seen in practically all jet aircraft. This signature was most evident as one watched TV clips of the Grenada intervention. In the decades to come, as the nation commences the use of alternate, heavier fuels and liquids derived from coal, shale oil, tar sands, etc., the soot problem will become even more severe. It is not surprising then that the understanding and control of soot formation and destruction have become one of the primary concerns of many investigators in the combustion field.

One of the major challenges with regard to soot formation has been to determine the sooting tendencies of various fuel types in order to be able to rank fuels and gain insights into the processes leading to soot formation. A significant contribution has recently evolved from work at Princeton University where it was shown that the effect of fuel type could not be determined without comparing various fuels at the same flame temperature [1]. Results from the Princeton effort made it evident that in diffusion-controlled systems that the higher the flame temperature the greater the tendency to soot and in pre-mixed combustion systems the reverse was true. From a practical point of view, diffusion flame systems are the most important as they exist most frequently in real engine configurations.

The Princeton work on sooting diffusion flames made use of a simple fuel jet operated in a highly overventilated state with air. The tendency of a fuel to soot was determined from the smoke point or soot height and the temperature effect was found by diluting the fuel jet with various amounts of nitrogen. The data obtained were plotted as the inverse of the mass flow at the smoke point versus the reciprocal of the calculated adiabatic flame temperature and each fuel plot was found to be a straight line. Having a straight line on such Arrhenius plots was some indication that fuel pyrolysis rates were the controlling element in the overall soot formation process.

This new conceptual approach to the soot problem drew a great deal of attention, for if a simple smoke height test in which the temperature was

controlled by nitrogen addition could tell the relative tendency of an individual fuel component to soot and its temperature sensitivity, then a powerful tool was at hand. Not only could a fuel be readily evaluated, but also by dealing with individual components, the effect of hydrocarbon structure could be evaluated. Such information could be invaluable in elucidating what the important soot precursors were. Questions then arose as to what explicitly the smoke height measured, was it indeed a true indicator of sooting tendency and was the calculated adiabatic flame temperature the proper correlating temperature in sooting diffusion flames. Intimately tied to these questions was what indeed was the structure of a sooting diffusion flame, what were the temperatures throughout the flame, was the stoichiometric temperature reached through a large portion of the flame front and, if not, was the temperature of the flame front close to the calculated adiabatic stoichiometric temperature or some large fraction of it. Obtaining answers to these points was one of the most challenging efforts in the soot formation field and it was immediately apparent that only by accurate measurement of the temperature field in the most adverse environment of a sooting flame could the proper foundation be laid.

Because of the general symmetry of a sooting, fuel-jet flame, the high temperatures existing and the presence of large concentrations of particulate matter, the only reliable means of obtaining accurate temperature measurement had to be some non-immersion optical technique. Indeed the only feasible technique that was known was coherent anti-Stokes Raman spectroscopy (CARS). Because UTRC was one of the leading developers of the CARS technique for combustion systems and Princeton had been one of the pioneers in interpreting sooting tendencies in diffusion-controlled combustion systems, UTRC and Princeton submitted a joint proposal to ONR in an effort to resolve the important dilemma described above and to contribute further to understanding the soot formation process. It became immediately evident that the results of the proposed study would have even more far reaching impact in that they could help resolve the important matter as to what explicitly was the structure of a jet diffusion flame. This fundamental result would have application not only with respect to the soot formation question, but to all diffusion flame systems in which particulates form. From the standpoint of the the Navy, such results could apply fundamental background to the study of a jet flame system which would come about by other particulate-laden combustion systems such as any of several metallic systems.

Summary of Major Results

This document is the final report of the ONR-supported joint effort. The findings have been most significant and though they are reviewed in detail in the subsequent sections they can be summarized as follows. For any significant sooting flame, the luminous flame height extends well past the

stoichiometric (Burke-Schumann) flame surface. The axial temperature profile of a laminar, fuel-jet flame increases to a maximum value which is well below the calculated stoichiometric adiabatic flame temperature and then decreases further. As the fuel jet is diluted, its axial temperature is at first less than its undiluted partner and then reaches a greater maximum value. This result is significant in that it indicates that the undiluted flame produces more soot which causes a greater radiation loss and thus a larger drop in temperature. Further, it means that soot must form in a region where the temperature field is higher than that of the diluted flame. Obviously this field is well below the flame tip. Scattering measuring determining particle densities, as well as the CARS temperature measurements substantiate these conclusions. Radial temperature measurements well below the flame tip show that the temperature at the flame edge (which is the radial maximum) is approximately 88% of the calculated adiabatic flame for sooting flames of various hydrocarbon fuels. Most interestingly, measurements on a carbon monoxide diffusion flame, which is non-sooting, also show its flame edge temperature to be 88% of the calculated values. Thus, one can conclude that the variation between the measured and calculated temperatures is not due to radiation losses, but more likely to finite reaction kinetics. It is not surprising then that there appears to be a fixed value between measured and calculated temperature no matter which fuel is used. This latter conclusion is most important in that it implies the use of the calculated temperature in the smoke height test has physical significance and can be considered a true parameter. The general conclusion then is that smoke height tests as used and correlated by the Princeton group have been verified fundamentally and is an appropriate means of evaluating any hydrocarbon species tendency to soot and its sooting temperature sensitivity. Thus, the procedure can be used to determine the effect of fuel structure on sooting and as a tool for searching out what the actual soot precursors really are.

As part of the overall program, Princeton University served as a subcontractor to UTRC. Princeton's function as a subcontractor to this research effort was two-fold: first, and primarily, to assist the diagnostics group at UTRC in the planning of the combustion experiments and in the analysis of the data obtained and, second, to construct a similar experiment in order to develop a technique of measuring soot particle velocities in a cylindrical flame. Such measurements would serve as another check of the validity of the simple Princeton smoke height test procedure in that it would measure a particular mass of soot formed to total fuel flow parameter as a function of the calculated adiabatic flame temperature. If the fuel trends correlated with this parameter were the same as those of the smoke height test, then again the smoke height test would have greater validity. Furthermore, velocity measurements would give greater understanding of the structure of a sooting diffusion flame.

Organization of Report

This final report is a management summary of the research performed jointly by UTRC and Princeton University. Those results which are ready for archival publication are reported on in considerably more detail in two technical reports [2,3] issued under the contract. They are also being submitted to archival scientific journals for publication. Some technical results which are not yet complete enough for a journal article are contained in Appendix A of this document. These results will become part of the Ph.D. dissertation of Mr. Allesandro Gomez, who was supported in part by this contract. The sections below summarize additional research performed under the contract. The considerable data base of temperature and particle size measurements and methodology improvements is being disseminated through verbal presentations, private communication, and publications.

APPARATUS DEVELOPMENT

The initial phases of this contract required that UTRC and Princeton have similar burners for the purpose of comparing new UTRC results with prior work at Princeton and to insure that new results from both contractors were directly comparable. To that end a Princeton graduate student, Allesandro Gomez, visited UTRC for almost four months. During this period he 1) assisted UTRC in designing and furnishing a burner similar to the one in use at Princeton, 2) provided UTRC with the Princeton design for a liquid fuel evaporator, 3) learned how to perform CARS calibrations and measurements so that their accuracy would be well understood by the people using them for soot formation modelling at Princeton, and 4) worked jointly with UTRC personnel in developing a calibration procedure for Mie scattering to be used at both places. Much effort was expended in improving flame stability by minimizing flame flicker. Also, calibration procedures were developed for the digital mass flow meters in use to assure their absolute calibration and the day-to-day reproducibility of flames. These efforts were necessary to assure the quality of the data to be obtained by both contractors. Burners were designed for the delivery of both gaseous and evaporated liquid fuels. The UTRC liquid fuel delivery system used a digital stepping motor driven liquid chromatography pump for flow delivery. The Princeton systems are described in Appendix A.

CARS MEASUREMENTS

This study was conceived shortly after Eckbreth and Hall [4] demonstrated the feasibility of performing CARS measurements in highly-sooting diffusion flames. While there are a few reports in the literature of comparisons between CARS and thermocouple measurements, to date this contract is the only known project where the goal was to use CARS as a bulk measurement technique. Because temperature was postulated at the time of the inception of this study to have a crucial role in soot formation in diffusion flames, it has been necessary to perform temperature measurements in as highly accurate a manner as the state-of-the-art would allow. Indeed, that the importance of temperature was successfully documented by this study, as described above in the introduction, is in large measure due to the use of the best available methods. While the original intent was not to develop CARS itself, some contract resources had to be expended in that area to address problems which arose. The serendipitous result is that not only was a temperature data base obtained, but also a number of improvements were made in CARS methodology. These improvements are expected to be of use to other CARS groups, especially when the device under observation is a practical device. A sooting diffusion flame is a considerable challenge due to the variety of conditions present. It is a system of sharp thermal gradients (hundreds of Kelvin/mm in certain regions), a system with great differences in chemical composition (fuel rich, fuel lean, combustion products), and a system in which the particulate loading

can vary from zero up to a troublesome volume fraction. Hence, what follows below is a record of a body of practical experience which was gained in performing CARS measurements in the variety of conditions present in different parts of a diffusion flame. Optical and other details of the apparatus are fully given in the first technical report [2].

CARS Data Acquisition

One of the first activities was the design of an glass chimney which would be suitable for not only the CARS temperature measurements but also the Mie scattering soot particle size measurements. The chimney had to be wide enough so that the converging laser beams would not damage the glass. The front and back sides had to be wide enough to accommodate the angle chosen for BOXCARS phase matching as well as allow movements of the burner perpendicular to the Stokes beam. Six side faces were chosen to allow Mie scattered light to be collected at three angles. Use of an irregular octagon kept the sides roughly perpendicular to the Mie beams. This minimized movement of the Mie focal spots as the table was translated.

Two problems became apparent once data collection was underway. First, due to the small size of some of the flames, especially the undiluted ones, the best spatial resolution obtainable was necessary. Unfortunately, there is a tradeoff between spatial resolution and signal strength. Hundreds of laser shots were already being averaged at the spatial resolution in use. Improvement of the spatial resolution meant even longer averaging times. Nevertheless, shorter focal length field lenses were installed in the system and the entire instrument realigned. While the shorter interaction length caused weaker signals it yielded the spatial resolution desired. The higher fields in the focal zone did, however, introduce some other complications which are described below. The second problem related to the efficiency of data collection. The original burner had hand-operated micrometers, which had to be painstakingly operated when the burner was moved for each data point. The manual position recording could also have led to possible errors. Hence, a contractor furnished stepping-motor-controlled, digital, three-axis translation system was installed. This unit was controlled by the laboratory computer and allowed absolute repositioning with 12.7 micron/step. Software was written to record the position automatically with the CARS spectrum. This unit was responsible for greatly increasing the number of data points which could be collected in a day.

Because of the small size of the flames being studied, convincing demonstrations of the spatial resolution were necessary. To measure the spatial resolution in the longitudinal (low resolution) direction, a glass cover slip was mounted to the burner and moved along the direction of beam propagation through the laser focal zone at low laser power. Since CARS light

is generated in the glass, a signal can be recorded which measures the length of the beam interaction region. It was determined to be about 0.7 mm for most of the data obtained under the contract. To measure the spatial resolution in the transverse (high resolution) direction the laser beams were attenuated and the beams cut by a knife edge moving through the waist of the focal zone. While beam refraction effects complicate this measurement, the transverse resolution was determined to be 0.1 - 0.15 mm. Optimization and calibration of the spectrograph and detector were achieved by placing a Xenon Penray lamp radiating through a pinhole in the CARS generation region.

One of the problems encountered with the shorter focal length system was saturation of the CARS signals. This distortion of the spectral shape is due to population pumping by the high laser fields. At moderate laser intensities, the CARS process does not affect energy level populations. Saturation causes the premature appearance of a hot band which if undetected causes the fitting routines to predict too high a temperature. It is most troublesome at low to moderate temperatures. Unfortunately, it is from room temperature spectra that various instrument parameters are determined such as the effective shape of the spectrometer slit (instrument function). This instrument function is then applied when fitting hotter spectra. Once it was determined that the focal zone fields were high enough to cause saturation it was scrupulously avoided by attenuating the laser pump beams. This unavoidably caused a lowering of the signal levels and consequent increase in the averaging time per data point. Since the highest possible accuracy was necessary, the spectra which were recorded early in the program were repeated. The early data base had, however, been quite qualitatively useful in formulating the detailed program plan.

Two other phenomena had to be avoided when working in fuel-rich regions of the diffusion flames. First, fuel molecules have a large polarizability which, in general, increases with molecular size. This lowers the electric breakdown threshold of the gas. At the high laser fields which were desirable for signal strength, certain of the fuel molecules under study allowed electrical breakdown (sparking) in the flames. The broadband emission from the breakdown plasma would be collected by the detection system and averaged in with the good CARS spectra obtained with laser pulses during which breakdown did not occur. When working in a fuel-rich zone the laser power had to be attenuated to eliminate breakdown.

Second, working in fuel-rich zones was more complicated due to the large and unknown third-order nonresonant susceptibility of the gas. The fuels under study have generally unknown susceptibilities, and to make matters

worse, undergo pyrolysis into smaller molecules. The smaller molecules have smaller and generally better known susceptibilities, but their concentration is at this point completely unknown. This problem is a data analysis rather than recording problem, and is discussed below in the CARS data analysis section.

Several problems were encountered for the most highly sooting fuels. Eckbreth had shown [5] shortly before the inception of this program that laser-modulated soot incandescence, anti-Stokes fluorescence, and electronically resonant CARS could cause interferences to CARS spectra when a Nd/YAG pump laser was used in combination with a broadband Stokes laser. Basically, in a region of heavy soot loading, a significant concentration of C_2 molecules can be produced by the rapid heating and volatilization of soot by the 10 ns laser pulse. This may manifest itself as signals which appear between the nitrogen CARS hot and cold bands. In order to minimize the effect of this signal a way of working was established where one of the BOXCARS pump beams is blocked and the level of detector dark count and interference signal is recorded in the presence of the remaining pump and Stokes beams. This background spectrum is then subtracted from the spectrum recorded with all three laser beams on. For most of the fuels this was an adequate procedure. For the most highly soot laden region of flames with a few of the fuels there was some interference still present. Fortunately, these were regions of mild temperature gradients and the absence of temperature data points in them was not a serious problem.

Another situation arose in the most highly sooting regions with certain fuels. The recorded spectra were highly distorted and at first it appeared that the background susceptibility might be unusually large in the presence of the C_2 . However, C_2 is a diatomic and should have a small susceptibility. We now tentatively ascribe this distortion to an absorption by C_2 in the cold band region which is strong enough to absorb a substantial amount of the signal--thus making it appear on normalizing the spectrum that the hot band and background are enhanced. It should be possible to perform an electronic absorption spectrum calculation for C_2 to help confirm this conjecture. For the current program it was possible to obtain temperatures from these spectra of reduced accuracy by fitting only the hot band portion of the spectra.

One early problem concerned the day to day reproducibility of measured temperatures. This problem was traced to daily, and sometimes hourly, changes in the spectral shape of the output of the Stokes laser. Some relief was obtained after the room was air conditioned for computer equipment and the dye solution was changed frequently. However, for insured accuracy dye spectra were recorded at least twice daily to be sure that the most current shape was applied in the data analysis. For efficiency in this regard, cold CO_2 gas was flowed through the burner tube and the focal zone placed at the burner lip, rather than inserting high pressure argon cells in the more conventional method.

CARS Temperature Calculations

Early in the program standard regression fitting on the central computer was used for fitting acquired spectra. After the computer-controlled burner translation table was installed, a considerable analysis backlog developed. Also, the computer intensive fitting methods employed were consuming an unacceptably large portion of program resources. Hence, for initial surveys with ethylene a number of quick-fit routines was devised for the laboratory minicomputer. This was before the difficulty of handling the background susceptibility in the central fuel core was fully appreciated. These quick-fit routines were crude but valuable in assuring that only archival quality spectra were submitted to the central computer for analysis and considerable cost savings. About that time the contractor-provided CARS laboratory VAX computer was delivered and made available to the program. This stand-alone computer was capable of receiving spectra from the acquisition minicomputer and processing the spectra by regression analysis as an overnight batch process. Hence, all further development of quick fitters for this program was abandoned and regression was used for all further analysis.

One of the analytical problems mentioned above was the difficulty of spectral analysis in regions of high susceptibility and unknown composition. This condition is present not only in the fuel core of the jet diffusion flames studied in this program but also in many practical devices such as gas turbine combustors and internal combustion engines. Under the current program a method was devised which uses two parameters. The first is, of course, the temperature and the second is the ratio of the resonant species concentration (nitrogen) to the generally unknown susceptibility. This method was fully reported by Hall and Boedeker [6] and is expected to be a significant contribution to the application of CARS to practical devices.

Summary

While understanding and solving the above problems consumed more program resources than was anticipated early in the program, the large data base with various fuels reported in the first [2] and second [3] technical reports attests to the continued viability of CARS as the only spectral technique available for the hot, luminous, particulate laden conditions found in hydrocarbon and other diffusion flames.

PARTICLE-SIZING MEASUREMENT IMPROVEMENTS

Because of the experience of UTRC in particle sizing by angular-dissymmetry Mie scattering [7], it was chosen as the method to be used for the current program. The alternate choice would have been extinction-scattering. The latter would have involved the installation of a cw laser with a collimated output beam and the writing of an Abel inversion computer program. There are multiple assumptions with either method and the former was selected on the basis of convenience and cost. It also provided the opportunity to demonstrate the feasibility of performing Mie scattering diagnosis with a pulsed laser--in fact, the same laser used for CARS with great attenuation. Both methods have been used by various workers before and the general correlation between results obtained by each is known. Extinction/scattering has historically given slightly smaller particle sizes and higher volume fractions than angular dissymmetry. Either method would be adequate for the relative comparison of different fuels or different flame conditions for the same fuel. Due to the assumptions involved, it is not currently known which method gives results closer to the absolute truth. The angular dissymmetry method and Mie scattering analysis does, however, allow the possibility of solving for the soot particle distribution width as well as mean. With extinction/scattering it has been usual to assume a monodisperse distribution and use the simpler Rayleigh scattering formulas.

Performance of the Mie measurements presented several technical challenges. First, it was not clear whether the flame stability was adequate for the performance of the Mie measurements subsequent to the CARS measurements, or whether it was necessary to intermix the two by automated attenuation of beam stops, attenuators, and polarizers. After the considerable effort on flame stabilization described above, the former, more expedient method was judged satisfactory. Second, it was necessary to devise a detection system which would have a spatial resolution comparable to the CARS spatial resolution and to assure that the two interaction regions overlapped. Third, it was necessary to suppress stray scattered light as much as possible and develop a method of absolute calibration of the received light intensity for the purpose of reporting absolute particle number densities. Finally, while UTRC had at its disposal a general purpose and well tested Mie scattering code, it was necessary to adapt that code to invert the experimental angular scattering data to give a number density and mean particle size. Normally, the latter are inputs to the code which calculates a scattering diagram for the input conditions.

Prior UTRC particle sizing apparatuses had used pinhole detector arms. Unfortunately, the infinite depth of field of these systems was not adequate for suppression of scattered light in the octagonal chimney system. Instead focussing beam systems were designed which would control the depth of field

well enough to assure that it was much smaller than the effective chimney radius. The resultant optical system had 1:1 imaging using 140 mm focal length lenses. The scattered light was collected from about a 2 degree angle in the scattering plane for each detector, collimated, and refocussed onto a single-fiber optical cable. This cable transmitted the collected light to a photomultiplier tube. The collimated section contained a rotatable polarizer and sometimes a neutral density filter. A narrowband interference filter was inserted at the entrance to the photomultiplier housing. The system thus had excellent rejection not only of stray light not at the laser wavelength but also of stray light at the laser wavelength. The polarizer made it easy to measure depolarization ratios as a further check on data quality. Since it is easier to calibrate neutral density filters than to measure the gain curve of a photomultiplier, the photomultipliers were operated at constant gain. All needed attenuation was obtained by inserting neutral density filters in the laser beam ahead of the scattering center. The diameter of the collection region was determined by the diameter of the optical fiber--about 0.6 mm. The length of the interaction region was determined by the focal width of the exciting beam--about 0.1 mm. The collection volume was thus approximately the same as the CARS interaction region.

It was necessary to assure that all three detectors collected light from the same scattering volume and that this volume was overlapped with the CARS volume as well as possible. This optical challenge was solved by mounting a stiff single quartz fiber to a brass plug which fit press fit the burner tube. This assured that the fiber was centered on the burner tube. The translation system was then moved to center the burner on the intersection of the two CARS pump laser beams. One of the beams was then blocked and the reflection of the other off the quartz fiber scattered light in the plane of the table. The angular position of the arms was accurately determined by pinholes mounted to a protractor on the burner plug. Glass flats simulated the optical effect of the chimney. Thus, light at the desired angles would be the only light to propagate toward the detectors. The optical fibers were then moved so that the focussed light from the quartz fiber would fall on the ends of the optical fibers. The separation of the collection lens from the scattering center and the refocussing lens from the optical fiber was first set to the lens nominal focal lengths and then optimized slightly for best focus.

Once the position of the detectors had been determined, it was necessary to adjust their sensitivity for the different optical throughput of the optical legs. The scattering from the quartz fiber could not be used for this task since it was not angularly uniform. Instead, Rayleigh scattering from pure gases was used. The gain of the detectors was set to a high level and the neutral density attenuation of the pump laser was adjusted to give Rayleigh scattering signals in the perpendicular polarization to the detectors. Their voltages were then trimmed to give uniform boxcar averager

signals. Further adjustments in sensitivity were made only with neutral density filters. The uniformity of the Rayleigh signals had to be checked with different gases flowing through the burner tube. This procedure was carried out for two gases of known and greatly different Rayleigh cross sections, carbon dioxide and helium. Efforts to remove stray light were continued until the known scattering ratio for these gases was obtained. This involved the design and installation of baffles and filters throughout the optical system. Once the Mie system was shown to yield adequate Rayleigh ratios it could be used to obtain soot scattering data. The Rayleigh signals were used as a check on detector balance before and after each Mie run. The absolute value of the Rayleigh signals also needed to be recorded for the purpose of ratioing the observed Mie signals to in. In this manner the absolute number density of soot particles could be recorded.

NUMERICAL MODELLING EFFORTS

It became clear early in the program that it would be instructive to compare the data base of temperature measurements being obtained with calculations and measurements of others. While the modelling effort at Princeton was concentrating on soot formation modelling, it became apparent that flame structure modelling should be done as well. Dr. Reggie Mitchell of the combustion research facility at Sandia National Laboratories had obtained [8], while at M.I.T., reasonable agreement between mass spectrometer and thermocouple temperature measurements in a methane diffusion flame and the predictions of a flame-sheet computer model. This model uses the Burke-Schumann flame sheet solution to the diffusion flame equations as its initial approximate solution and then numerically regresses to a better solution under relaxed assumptions. He kindly made the methane version of this code running on the Cray computer at Sandia available to UTRC. UTRC then modified this code for the same laboratory VAX computer described above and changed the thermodynamic and transport properties throughout the code to adapt it to ethylene. A single case consumed about 12 hours of CPU time on the laboratory VAX and such calculations were run overnight.

In spite of the severe assumptions and one-step diffusion-controlled chemistry in this code, its use was quite valuable to the research program in providing qualitative insights into the measurements. One diagnostic apparatus which was not part of the current program at UTRC was LDV for measurement of flame velocities. Since the flames under study are buoyancy dominated the velocity predictions of the program were informative in understanding the approximate direction of streamlines. Another benefit of the program's use arose in comparing undiluted flames with their nitrogen-diluted counterparts at constant fuel flow. While the model, in agreement with theory, predicted only a modest lengthening of the combustion zone on addition of diluent, the luminous heights decreased substantially in the experiment. From this important dichotomy it became clear that there were many unresolved questions about flame structure being raised by this research. While Mitchell did not observe a large difference between the luminous zone and the calculated combustion zone for methane, methane is a less sooting fuel and smaller molecule than ethylene. The detailed comparison between the predictions of this code and the measurements obtained in this program may be found in the two technical reports [2,3].

VELOCITY DIAGNOSTICS

One of the activities of Princeton University was to guide UTRC on the proper and relevant experiments which should be performed with the existing apparatus. Since velocity information would be extremely valuable in answering certain questions about soot breakthrough, and as part of the graduate work of Mr. Allesandro Gomez, who was supported by this program, a series of tests was performed to see if a simple velocity diagnostic could be devised which would be of benefit to the current program. Breakthrough is an important component in the Princeton model for fuel structure effects on soot formation. It is the so-called "sooting height"--or onset of smoke production--which is used to rank the sooting tendencies of fuels.

The selection of the pulsed laser allows great flexibility lending itself to future spectroscopic studies. However, it has one drawback: it does not allow the application of LDV techniques because of the very short laser pulses. Therefore, it was necessary to resort to alternative non-intrusive techniques.

A laser enhanced ionization technique [9] was first attempted. Briefly, sodium atoms were seeded into the fuel flow and were excited in the flame with the dye laser tuned to the atoms' resonance transition. When the atoms concentration is sufficiently high, associative ionization occurs, due to excited molecule-excited molecule collisions. Light from a sodium lamp focused in the flame downstream of the pulsed laser was collected in extinction by a photodiode. When a cloud of reduced neutral atoms concentration reaches the extinction line of the sodium lamp, a reduction in the extinction signal should be noticed as a pulse on an oscilloscope. Knowing the distance between the pulsed laser beam and the extinction line, one can determine an average velocity in the region by measuring time of flight of the cloud between the two points.

The technique had been employed by other investigators for parallel beams. In the present situation, however, spatial resolution constraints imposed a fairly large angle between the pulsed beam and the "probe" line. Since the extinction is a line of sight measurement, changes in a small region of the extinction line, determined by the traveling cloud, were not noticeable on the oscilloscope. Consequently, no ionization signal was detected by this technique, except when the extinction line was replaced by an ionization probe.

Since it was deemed important to keep the diagnostics non-intrusive in the small volumes to be sampled, a second technique based on the laser vaporization of soot [10] was attempted. The high energy flux associated with the tightly focused pulsed laser beam causes vaporization of the soot

particles with consequent reduction of light scattering and extinction. An He-Ne laser aligned a known distance downstream of the pulsed beam was focused on a photodiode. By measuring the time delay between pulse generation and the observation of a decrease in the probe extinction, the average velocity in a small volume can be determined.

This technique allows the determination of one component of the velocity, only in particulate laden flows. By measuring the velocity on the flame axis and interpolating between the burner rim, where the gas velocity is known from mass conservation and a thermocouple measurement, and the first point where soot is present on the axis, one can evaluate residence times for comparisons among different flame conditions and different classes of fuels.

The technique was successfully applied to a butene flame; velocities between 0.6 and 1.2 m/s were measured in preliminary experiments. While this result is encouraging for further future development of this technique, it was judged too far from reduction to everyday practice for use on the current program. It remains, however, a significant technical result for future development in particulate-laden systems in which the particles are vaporizable.

DATA BASE

Once the experimental challenges had been met and it was judged that the data being obtained were correct in an absolute sense at the current state of the art, it was possible to collect a large data base of CARS and Mie scattering data. The size of the data base and its efficient processing were due in part to the availability of a highly reproducible flow system, a burner translation system with excellent spatial resolution and reproducibility, complete computer automated recording of virtually all necessary voltages, spectra, calibration factors, etc., and the development of "batch" analysis command procedures for the laboratory VAX which could take a large series of runs and analyze and plot the results without much manual manipulation. This process was overseen, however, by a vigilant scrutiny of the process which assured the quality of the final result. Indeed, where experimental difficulties or inconsistencies were found it was necessary to discard or repeat some of the data points to assure its ultimate utility.

CARS Measurements

While, in accordance with the program plan, a large part of the temperature data base was obtained with ethylene fuel under a variety of conditions, data were also obtained with other fuels of considerably different structure. Some prior measurements of Eckbreth and Hall [4] in propane were repeated due to the importance with which they were being taken by soot formation modellers. The purpose of their landmark study was merely to show that CARS temperature measurements could be done in highly-sooting flames. The high temperatures in that paper reflected the state of the art in 1977 in CARS measurements. In the interim period there were improvements in spectral constants, computer rather than visual fitting began to be used, and the two-dimensional fitting procedure for handling fuel-rich regions was developed--the latter under the current program. The importance of the result to modellers required that the measurements be repeated with use of the improved methods. Indeed, the measured temperatures were substantially reduced and the revised values reported at the Twentieth International Symposium on Combustion [12] and also at the Eastern States Meeting [13].

The largest body of CARS measurements was obtained with ethylene fuel. Originally, it was planned to study ethylene to compare with prior work at Princeton. It became apparent, however, that ethylene would be far more important in elucidating a soot model. It was discovered that in a series of undiluted and nitrogen-diluted ethylene flames that the upper parts of the diluted flames were hotter than their undiluted counterparts. This surprising result provoked a lengthy examination of our procedures and repetition of many data points. We now explain this result by postulating that 1) the fuel flame front is well inside the luminous zone, in accordance with the predictions of

the numerical model, and 2) that there is a large heat loss from the system due to blackbody radiation from the soot particles. Hence, the upper part of the flame is a burnout region in which oxidant must be present. These results and their significance are explained in far more detail in the first technical report [2].

To be sure of the adequacy of the two-parameter fitting technique being used for the fuel-rich part of the flame and to address the question of whether the inversions observed could be due to finite-rate chemistry instead of radiation, surveys were conducted in a CO flame. In CO there is no pyrolysis of the fuel and no soot formation. The third-order nonresonant susceptibility is also known much better for CO than ethylene. The CO work confirmed that even soot-free flames do not reach their adiabatic flame temperature, and that there was no inversion of the temperature curves for undiluted and diluted CO flames.

Temperature profiles were also obtained in fuels of comparatively different structure. In order to not deplete program resources, these surveys were more limited than the complete mapping attempted with ethylene. Nevertheless, enough data were obtained for each fuel to show that the same kind of temperature inversion observed with ethylene is observed in other fuels. Further, enough data were obtained at the same positions where particle size distribution data were obtained to allow correlation inferences to be made. The C₂ fuels studied were a double-bonded alkene, ethylene (C₂H₄), and a triple-bonded alkyne, acetylene (C₂H₂). The C₃ fuels were a saturated alkane, propane (C₃H₈), and an unsaturated alkene in which there is no conjugation, allene (C₃H₄). The C₄ fuels were an unconjugated alkene, 1-butene (C₄H₈), and a conjugated diene, 1,3-butadiene (C₄H₆). For some of these highly-sooting fuels it was a considerable challenge to obtain data due to their small sooting heights. They also displayed some of the C₂ interferences described above. Nevertheless it was possible to compare diluted flames with undiluted ones, and smoke-height flames with flames not at the smoke height. The details of this survey may be found in Technical Report 2 [3].

Mie measurements

For the same reasons given above for the CARS measurements in regard to the discovered importance of radiation effects, the bulk of the angular dissymmetry particle sizing data base is on diluted and undiluted ethylene flames. Scattering data were also obtained for the same variety of fuels and conditions described above. The temperature/soot correlations discovered in this survey are discussed in Technical Report 2 [3].

RESULTS AND DISCUSSION

This UTRC/Princeton program on sooting diffusion flames produced significant fundamental results which not only helped verify the validity of the simple Princeton smoke height test as a method for ranking the sooting tendency of fuels, but also to define the structure and characteristics of diffusion flames in which particulates are a major species component. This latter aspect has particular significance as well in defining the structure of particulate-laden diffusion flames in which either a hydrocarbon or a metallic substance is the fuel.

The complete understanding of sooting diffusion flame hinges not only on the ability to measure mean particle sizes and particle volume concentrations, as many have done, but also on the ability to accurately measure the temperature distribution throughout the diffusion flame. Such measurements have been performed during the current program and a significant data base established. The CARS techniques and particle scattering techniques techniques have been verified on laminar gaseous fuel jets and can now serve to answer many unknowns on particulate-laden flame structure.

Summarized below are some of the basic conclusions and technical contributions of the technical program. For specific justifications of the conclusions and more information about their limits of applicability, the two technical reports [2,3] should be consulted. Some of the technical contributions of the program to laser diagnostics have been discussed above.

Soot-Formation

It was demonstrated early in the program that temperature has a large effect on diffusion flame soot formation. Indeed for many of the flames studied, soot formation could be altogether suppressed by lowering the temperature with diluent. Comparing undiluted and diluted flames at constant fuel flow, it was found that low in the flame the flames have the expected ordering: the most diluted flame is coolest. However, the surprising result was obtained that at the top of the same flames the most diluted flame was hottest. This unexpected phenomenon was ascribed to the influence of radiation as a heat loss. Low in the flame the diluent controls the rate of pyrolysis in the fuel core and thereby influences the production of soot precursors.

At the flame front low in the flame, soot is formed if the maximum radial temperature is high enough. The rate of production at the flame front appears to be directly relatable to the adiabatic flame temperature of the system--hence the importance of the AFT in determining the smoke height for a given fuel. However, in the less dilute flames the number of soot particles formed is large due to the high temperature low in the flame--and the hot particles are free to radiate energy away from the flame. Hence the upper

parts of such flames appear relatively cool. The CO flame results (in which there is no pyrolysis or soot) show no temperature curve crossings. The CO flames also show that the maximum radial temperature scales with the AFT. These results together provide insight into the physical basis of the Glassman smoke height correlation [1]. Nevertheless, there are many unanswered questions regarding the details of the temperature/soot correlations observed and the behavior of different fuels--especially acetylene. One of the most interesting correlations which was observed, however, is that the tip temperature of smoke height flames of different fuels is the same to within about 100 K. This temperature appears to be the threshold temperature for burnup of soot particles. When the fuel combustion zone (see below) is sufficiently far from the tip, the heat release is insufficient to maintain combustion.

Flame Structure

One of the most exciting aspects of the current program was the large number of flame structure questions which arose. Our current picture of a hydrocarbon diffusion flame is quite different from the model in use at the inception of the program. Further definitive work on these questions could lead to general results which are applicable to a wide variety of particulate-laden diffusion flames.

It became clear that, while generalizations could be made based on the adiabatic flame temperature, that these systems were far from adiabatic. Early temperature measurements led to the observation that short, low flow rate flames reached a lower overall fraction of the fuel AFT than higher flow rate flames. This heat loss was ascribed to the influence of the burner. The support structure not only conducts away thermal energy from the system, it also redistributes it by preheating the fuel. These attributes lower the overall temperature by removing heat, but can accelerate pyrolysis if the fuel preheating is severe enough. Also, the burner lip influence pyrolysis and soot formation by allowing oxidant to diffuse into the pyrolysis region. A small amount of oxygen can catalyze pyrolysis. Different lip shapes influenced the extent of the blue zone which precedes soot luminosity. At their current state of development numerical models of diffusion flames neglect burner heat loss and burner fine-scale aerodynamic effects. They also neglect soot formation, mass transport, radiation, and burnup.

A great deal of circumstantial evidence from the current program points to soot radiation as a heat loss mechanism. The role this plays in affecting the chemistry of soot production and burnup is now understood to be much greater than was anticipated at the program start. Nevertheless, there was not the opportunity in the current program to perform quantitative external radiation measurements. Such measurements would allow a correlation of the implied heat flux with a radiaton model based on internal measurements.

One of the most important results from the current program is the implication that the fuel combustion flame front (as in a Burke-Schumann flame sheet model) is well inside the luminous flame in the upper part. Low in the flame the soot annulus is inside the flame front as expected. However the fuel flame length is considerably shorter than the luminous height, and the flame surface must cross the soot surface. The entire upper region of the flame is now pictured as a soot burnout zone in which oxidant is present. The numerical model discussed above was very useful in understanding this behaviour and the fact that the fuel flame length increases only slightly on addition of diluent--while the visible height shortens.

Soot formation was shown to be highly dependent on temperature. This is due to the sensitivity of the formation and growth kinetics on the rate of fuel pyrolysis. It was not part of the current program to try to measure directly the rate of fuel pyrolysis, but several strategies exist employing the species detection capabilities of CARS for such a measurement.

AREAS FOR FUTURE WORK

While the current program contributed greatly to our understanding of the physical basis of diffusion flame soot formation and flame structure, it obviously left many questions hanging which could be addressed by laser diagnostics. There are several general areas in which successor programs could concentrate. One rather obvious area would be a continuation of the same areas of inquiry taking advantage of recent diagnostic developments for species detection and adding, for example, LDV diagnosis of gas velocity. This would allow computation of the absolute soot flux throughout the flame. Such a program might include improvements to numerical models of soot formation to include burner and radiative heat losses, as well as soot formation, growth, and destruction.

Another general area would be to investigate the applicability of the laminar model to more turbulent situations. While we believe that the general principles determined for the laminar flames are at least qualitatively useful for turbulent, practical devices, it remains to be shown definitively. A program in which controlled perturbations were introduced, while flame and soot characteristics are monitored with laser diagnostics, could begin to address this question.

Finally, the flame structure findings and questions uncovered in this program should be characteristic of particulate-laden flames in general. While phenomena such as burnout might be absent, metal-fueled flames producing oxide particles would be excellent candidates for examination.

REFERENCES

1. Glassman, I., Brezinsky, T., Gomez, A., and Takahashi, F., "Physical and Chemical Effects in Soot Formation" in *Recent Advances in Aerospace Science*, Ed. by C. Casci, Plenum Press, N.Y., 1984.
2. Boedeker, L. R., and Dobbs, G. M., "CARS Temperature Measurements in Sooting, Laminar Diffusion Flames", Technical Report No. 1, Contract N00014-81-C-0046, United Technologies Research Center, November, 1984.
3. Boedeker, L. R., and Dobbs, G. M., "Temperature and Soot Correlations in Sooting, Laminar Diffusion Flames", Technical Report No. 2, Contract N00014-81-C-0046, United Technologies Research Center, November, 1984.
4. Eckbreth, A. C. and Hall, R. J., "CARS Thermometry in a Sooting Flame", *Combustion and Flame* 36, 87-98 (1979).
5. Eckbreth, A. C., "CARS Investigations in Sooting and Turbulent Flames", Technical Report, Contract N00014-75-C1143, United Technologies Research Center, February, 1979.
6. Hall, R. J., and Boedeker, L. R., "CARS Thermometry in Fuel-rich Combustion Zones", *Applied Optics* 23, 1340-1346 (1984).
7. Bonczyk, P. A., "Measurement of Particulate Size by *in situ* Laser-Optical Methods: A Critical Evaluation Applied to Fuel-Pyrolyzed Carbon", *Combustion and Flame* 35, 191-206 (1979).
8. Mitchell, R. E., Sarofim, A. F., and Clomburg, L. A., "Experimental and Numerical Investigation of Confined Laminar Diffusion Flames", *Combustion and Flame* 37, 227-244 (1980).
9. Schenck, P. K., Travis, J. C., Turk, G. C. and O'Haver, T. C., "Laser-enhanced Ionization Flame Velocimeter", *Applied Spectroscopy* 36, 168-171 (1982).
10. Dasch, C. J., "New Soot Diagnostics in Flames Based on Laser Vaporization of Soot", Paper 131, Twentieth Symposium (International) on Combustion, Ann Arbor, Michigan, 12-17 August, 1984.
11. Gomez, A., Sidebotham, G. and Glassman, I., "Sooting Behavior in Temperature-Controlled Laminar Diffusion Flames", *Combust. Flame* 58, 45-57 (1984).

12. Boedeker, L. R., and Dobbs, G. M., "CARS Temperature Measurements in Sooting, Laminar Diffusion Flames", Paper PS67, Twentieth Symposium (International) on Combustion, Ann Arbor, Michigan, 12-17 August, 1984.
13. Dobbs, G. M., Boedeker, L. R., and Eckbreth, A. C., "Temperature and Soot Correlations in Sooting, Laminar Diffusion Flames", Paper 96, 1984 Technical Meeting, The Eastern Section of the Combustion Institute, Clearwater Beach, Florida, December 3-5, 1984.

APPENDIX A - PARTICLES SIZING IN DIFFUSION FLAMES

INTRODUCTION

This Appendix contains some experimental results, not yet reported elsewhere, which were obtained by Mr. Allesandro Gomez, a Ph.D. candidate at Princeton University. Acquisition of this data base was supported by this contract. The balance of his Ph.D. dissertation will be in part a theoretical assessment of these results. It is anticipated that these results will form the basis for an archival journal publication as well as be included in his dissertation. The particle sizing measurements reported are important for assessing the onset of sooting in some of the most heavily sooting flames. They therefore concentrate on the small particle regime where the particles are barely detectable and also on liquid fuels. As such they form a necessary complement to the work at UTRC which is summarized in the main body of this report.

Subsections below report on the particle sizing apparatus and method for small particles and the liquid fuel delivery systems.

EXPERIMENTAL ARRANGEMENT

The experimental apparatus, comprising essentially the burner and the liquid fuel vaporization system, is shown in Fig. A-1.

The burner consisted of two concentric tubes: fuel and diluent flowed through the inner one, a stainless steel tube measuring 10 mm i.d. and 700 mm in length and air was forced through the outer annulus whose confining brass tube measured 120 mm i.d. The air passage was filled with 3.0 mm glass beads and contained in its final section a stainless steel honeycomb that ensured streamlines parallel to those of the flow from the inner tube. In order to shield the flame from air draughts, an aluminum chimney with octagonal cross section was mounted on the burner housing; rectangular pyrex windows on the chimney allowed optical access to the flame. Gaseous flow rates were monitored by means of rotameters and eventually measured by a soap film meter.

Liquid fuels were vaporized using the following technique. Fuel stored in a stainless steel reservoir was pressurized by regulated nitrogen and forced into the evaporator through a 300 mm long, .150 mm i.d., stainless steel capillary tube. The evaporator consisted of a 10 cm long stainless steel porous cylinder encapsulated in a 13 mm i.d. stainless steel tube wound with heating wire. The high porosity of the cylinder enhanced the contact of liquid and hot surface within a relatively small volume; a preheated stream of nitrogen swept the hydrocarbon vapor into the burner. This design ensured good controllability and response of the system.

Fuel flow rates were controlled by varying the stagnation pressure in the fuel reservoir. At the small liquid flow rates of operation, Hagen-Poiseuille flow was established in the capillary, so that the volumetric flow rate was directly proportional to the pressure drop across the capillary. Since essentially all the pressure drop in the line was determined by the capillary, it was sufficient to measure the stagnation pressure in the fuel tank by a mercury manometer and later, off line, obtain volumetric flow rates by calibration of the system, using glass microburettes. During operation with these condensable mixtures all lines were heated to approximately 40 K above the fuel boiling point. Thermocouples measured all appropriate temperatures necessary to determine flow rates.

SCATTERING DIAGNOSTICS

Optical Configuration

A schematic of the optical instrumentation is shown in Fig. A-2. A N_2 laser pumped an organic dye; the dye laser, tuned to the appropriate wavelength, was directed to the burner. Photomultiplier tubes collected scattered light at three angles and a photodiode measured the transmitted intensity through the flame.

The N_2 laser pulse, with .2 MW peak power and 5 ns duration, was focussed through two cylindrical quartz lenses to transversely pump a 10 mm quartz cuvette filled with a dye solution. A magnetic stirrer was mounted below the dye cell to minimize optical saturation of the dye. The dye cavity configuration is the one suggested by Myers [A-1]. A 60° glass prism set for an angle of incidence close to 90° performs the function of beam expander. A 1200 line/mm diffraction grating used in first order Littrow mount provides a means of tuning the wavelength and narrowing the linewidth. Output coupling takes place through the reflection from the prism surface; the wavelength is tuned by rotating the diffraction grating. This configuration results in the best compromise of linewidth and cavity efficiency requirements: a linewidth of about .1 nm and a conversion efficiency of 15 % were obtained.

Part of the laser beam was deflected by a microscope slide onto a reference photodiode, before crossing the burner, in order to properly reference the data by taking into account laser power fluctuations. Polarization purity of the laser beam was ensured by using a Glan-Air polarizer mounted just before the focusing lens, a 150 mm focal length achromat, which produced a beam waist of 0.150 mm. After passing through the flame, the laser beam was refocussed onto a diffuser mounted on a photodiode

to measure the extinction from the flame. The light impinging the photodiode was attenuated to acceptable levels by a stack of neutral density filters.

The scattering signal was collected at 45°, 90° and 135° by plano-convex lenses of 141 mm focal length and refocussed onto a .2 mm pinhole by identical lenses. A rotatable dichroic sheet polarizer was mounted between the two lenses on each channel. Neutral density filters were inserted through three slots between the pinhole and the photomultiplier tube to keep the signal level within the linear range of the tube. The scattered light was filtered by a 1 nm FWHM interference filter centered at 530 nm, the selected wavelength for the scattering measurements.

Data Acquisition System

Scattering and extinction signals were processed by a gated integrator. The gated integrator was purchased as module cards and assembled together with a time delay module, triggered by a photodiode signal from the dye cavity, in order to avoid jitter between the laser pulse and the generated gate.

The output of the integrator was digitized by serial A/D converters which, in turn, were interfaced with a Commodore C-64 computer for data storage on diskettes. The C-64 was also programmed to drive two stepper motors, thus allowing an automated scanning and sampling of the flame in the radial and vertical direction. Data stored on diskettes were finally transferred to an HP-1000 for the final data reduction and plotting.

Data Analysis

The ratio of the transmitted laser intensity to the initial intensity for propagation through a collection of particles of uniform sizes and number density is given by

$$\tau = \frac{I}{I_0} = \exp \left(- \int_{r_1}^{r_2} N C_{\text{ext}} dr \right) \quad (\text{A-1})$$

where C_{ext} is an extinction cross-section, N is a particle number density and $r_2 - r_1$ is the physical length over which extinction takes place. Since the measured transmittance is the integrated value of the local extinction coefficients along the optical path through the flame, these data need to be inverted in order to yield the local values. To this end, a Fourier convolution technique was used, a method extensively documented in the literature [A-2].

The scattering intensity is proportional to the product of the scattering cross-section, particle number density, and incident light intensity,

$$I_{\text{scatt}} = K \sigma(\theta, d, \tilde{m}) N I_0 \quad (\text{A-2})$$

where σ is the scattering cross-section, d is the particle size, θ is the scattering angle, and \tilde{m} is the complex refractive index of the scattering particle. The constant K was determined by measuring Rayleigh scattering from flowing nitrogen and propane at ambient conditions. Scattering from flowing helium, which has a much smaller Rayleigh scattering cross-section, was measured to ensure that no stray light was detected from other sources. Since I_0 referred to the incident light at the scattering volume, which in highly sooting environments can be significantly different from the incident laser intensity before the flame, it was necessary to account properly for both the attenuation of the laser before the scattering volume and the attenuation of the scattered light between the scattering volume and the detector, by using the inverted extinction coefficients.

A code was implemented for the calculation of scattering and extinction cross-section for spherical particles in accordance with Mie-Lorentz theory. It was validated against published tables of real and complex Bessel functions [A-3], which are the main computational difficulty, and the agreement was within the fourth significant digit throughout the size range of interest. The calculations were made for a monodisperse distribution of particles.

Particle characteristics can, in principle, be determined in several ways:

- a. ratioing a scattering signal at, say, 90° for vertically polarized incident light and vertically polarized scattered light, Q_{vv} , and the extinction signal yields the determination of particle size for a given index of refraction. Knowing the particle size one can determine the scattering cross-section at that angle upon comparison with the calculated ratios and from (A-2) the number density. Then, volume fraction can be readily computed for spherical monodisperse particles.
- b. ratioing two scattering signals at, say, 45° and 135° (dissymmetry ratio). This allows the determination of particle sizes since N cancels out. Knowing the particle size one can proceed as in a.
- c. ratioing at 90° the horizontally polarized light for horizontally polarized incident light, Q_{hh} , over Q_{vv} at the same angle (polarization ratio).

In principle, methods (b) and (c) are more appealing in the present geometrical configuration since they yield directly point measurements, without the uncertainties associated with the inversion technique. In particular, it was originally planned, after some preliminary calculations, to use $Q_{vv}(45^\circ)/Q_{vv}(135^\circ)$ for particles in the large size range and $Q_{hh}(90^\circ)/Q_{vv}(90^\circ)$ for those in the small size range, which could allow mapping of the whole flame.

However, some problems arose from the use of the polarization ratio. First, it was noticed that there is an extreme sensitivity of Q_{hh} to the angular position around 90° , where the polarization ratio needs to be measured in order to have large sensitivity to particle size. Consequently, since the collection optics have a finite collection angle, the scattering signal is integrated over that angle. Calculations showed that it was necessary to reduce the aperture in front of the collecting lenses to 1 sr in order to preserve size sensitivity down to roughly 30 nm. However, even by doing so, the ratios of the detected signals in a flame were never lower than .5 %, corresponding to an unrealistically large particle size of 130 nm for monodisperse distribution. It was therefore concluded in accordance with other investigators' findings [A-5], that the technique is not applicable to soot particles because of their intrinsic optical anisotropy. In fact, the size effect is not clearly distinguishable from particle anisotropy effect in the measurement of Q_{hh} , since the depolarized scattering intensity is of the same order of magnitude of Q_{hh} . Since the dissymmetry ratio technique could not have allowed mapping of the entire flame, it was decided to resort to the scattering/extinction method for which some data will be presented. Supplementing these measurements with dissymmetry ratio data could provide, to some extent, information on particle size distribution parameters for a size distribution chosen a priori, as well as data in regions of the flame close to the tip where extinction would be immeasurably small.

RESULTS

Two fuels were tested: 1-butene and benzene. Experiments were performed at smoke height conditions, i.e. at the minimum height beyond which smoke just broke through the flame [A-8]. Two flames of 1-butene were examined: 1) an undiluted flame, characterized by a fuel volumetric flow rate of 0.413 cc/sec and a flame height of 23 mm; and 2) a diluted flame, in which N_2 was added to the fuel side in order to affect the flame temperature and the fuel flow rate was adjusted in order to restore smoke height conditions. In this second condition, the N_2/C_4H_8 molar ratio was 2.20 and the flame height was 44 mm. One experimental condition was studied for benzene: the N_2/C_6H_6 molar ratio was 2.55 and the flame height was 10 mm.

A NASA CEC program calculated the adiabatic stoichiometric flame temperature in air, properly adjusted for N_2 dilution, for all three flames. The calculated values were: 2327 K for the undiluted butene flame, 2253 K for the diluted butene condition and 2287 K for the diluted benzene flame.

Particle diameter, number density and volume fraction for the three flames are shown in Figs. A-3 to A-14.

The data are plotted as function of the radial coordinate, for selected values of an axial coordinate nondimensionalized with respect to the flame height. The flames exhibit the characteristic toroidal structure reported by other investigators [A-9] in the lower region, where intense nucleation as well as agglomeration yield quite large particle sizes, around 80 nm a few millimeters away from the burner lip. The main differences between the flames in this region occur near the centerline, and they could possibly be accounted for by the differences in the flow patterns of the three flames. In fact, if the soot noticed early on the centerline is convected in from the formation region closer to the flame surface, the higher will be the fuel jet momentum, the later the streamlines will converge toward the axis. Therefore, soot is observed on the flame axis earlier for flames with lower momentum, noticeably benzene.

Measured particle sizes, shown in Figs. A-3 to A-6, range between 15 nm toward 100 nm for all fuels, with no significant variations in the trends among the different flame conditions.

Volume fractions are shown in Figs. A-7 to A-10. Comparing the two butene flames in Figs. A-7 and A-8, it is noticed that the diluted flame exhibits consistently lower volume fractions except perhaps in the upper region of the flames. Furthermore, Fig. A-8 shows decreasing volume fraction as a function of the non-dimensionalized height, indicating that soot oxidation is dominant in this region.

Analogous trends are observable in Figs. A-9 and A-10, in which the undiluted butene flame is compared with the moderately diluted benzene flame. The benzene flame has consistently higher volume fractions than the butene flame at comparable nondimensionalized height. Knowing the fundamental role of temperature on sooting tendency of fuels in diffusion flames [A-8], one would expect that this difference would have been even more drastic if adiabatic flame temperatures had been closely matched.

Given the similarities in the trends and ranges of particle size between the flames, it is not surprising that the difference in volume fractions can be accounted for mainly by number density variations, as shown in Figs. A-11

to A-14. The region of highest number density at any axial location is close to the luminous flame envelope. It is interesting to notice that at the radial location when the number density attains a minimum in the lower region of the flame, volume fractions and particle sizes reach a maximum, as a consequence of strong surface growth and agglomeration processes. It is not clear whether there is soot formation around the centerline of the flames or if particles are carried into that region by convective-diffusive processes.

CONCLUSIONS

The experimental results seem to suggest that the smoke height is a more quantitative measurement than originally expected since the soot loading of the flames scales quite well with smoke height classification of fuels [A-8]. Number density variation account for most of the soot loading difference between flames. Experiments are underway on other flame conditions, with closely matched adiabatic flame temperatures, and different fuels. Velocity measurements on centerline should give some information about residence time effects, which should be taken into account in comparing different flames.

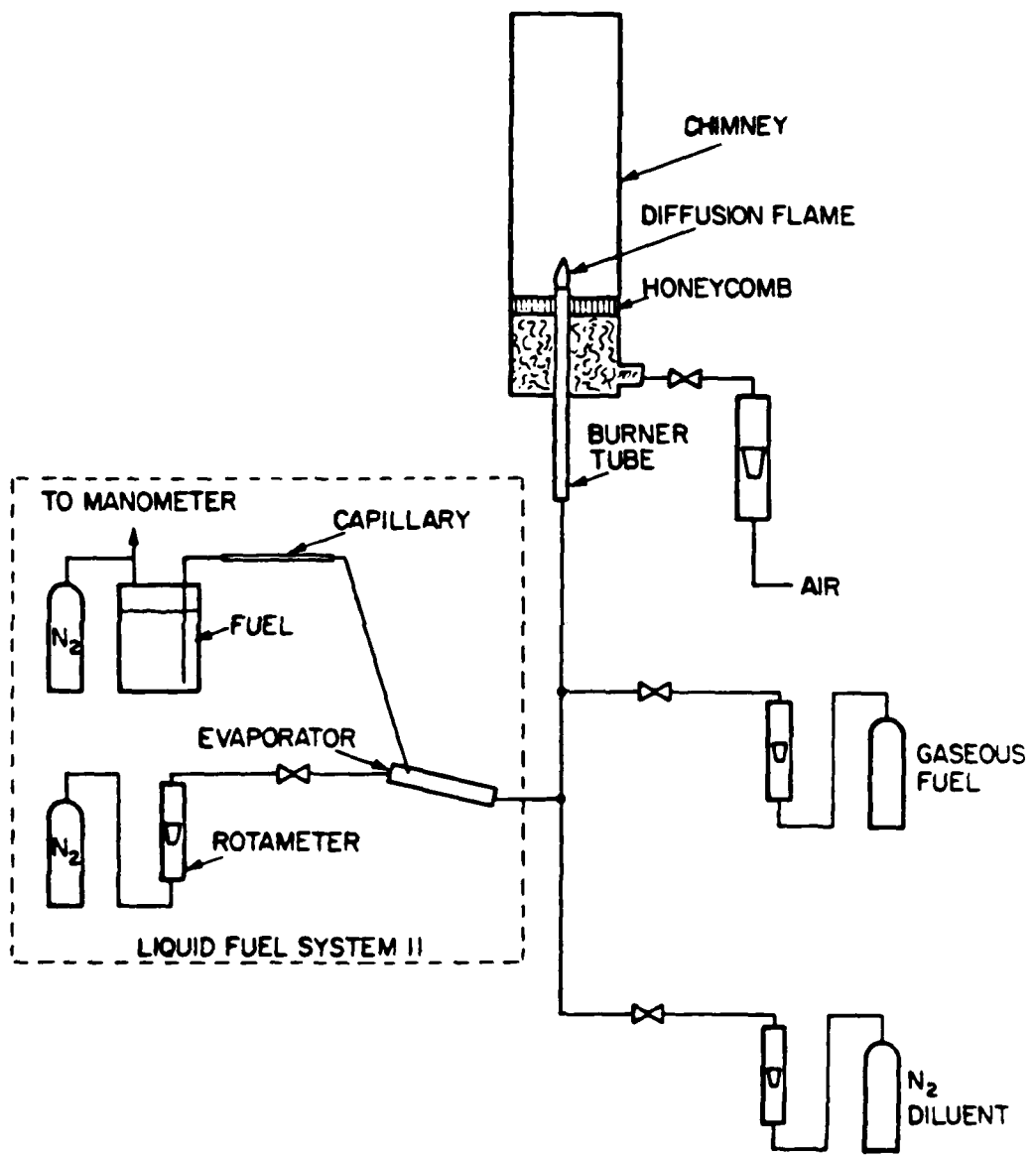


Figure A-1. Schematic of diffusion flame apparatus.

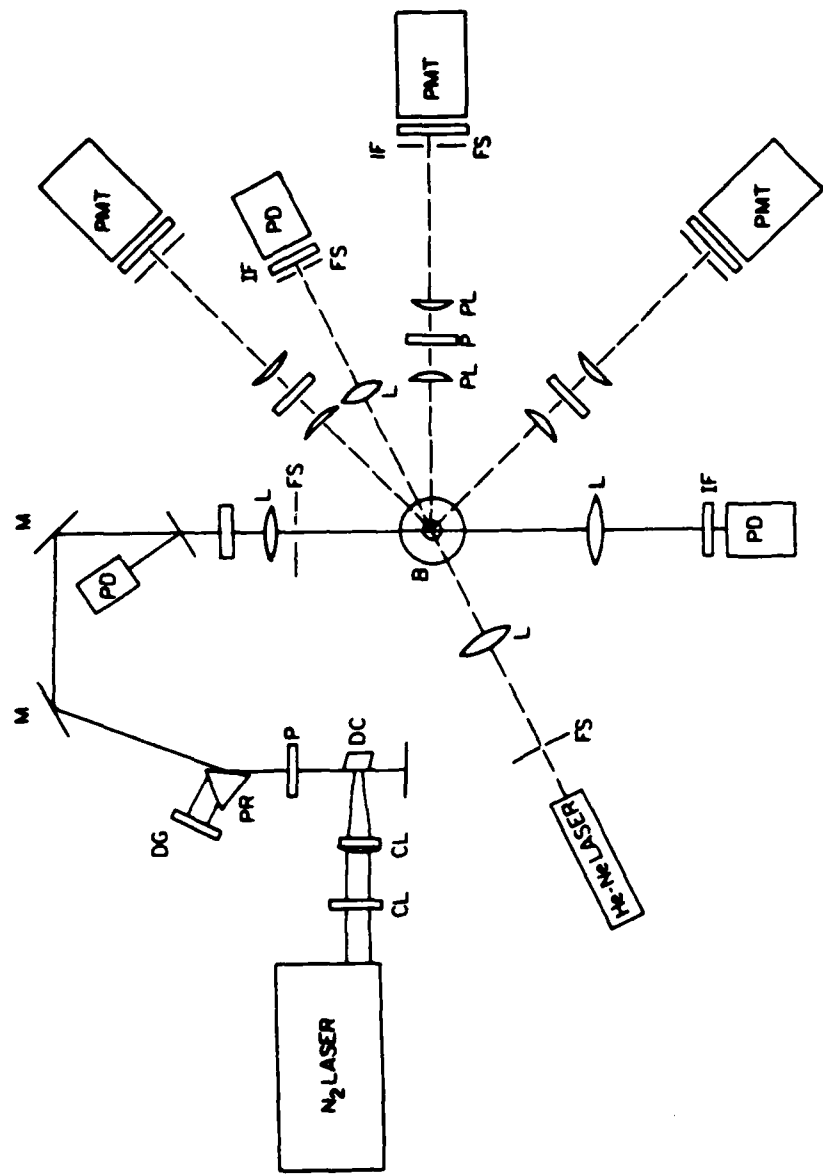


Figure A-2. Optical configuration CL - cylindrical lens; DC - dye cell; P - polarizer; PR - prism; DG - diffraction grating; M- mirror; L - lens; FS - field stop; IF - interference filter; PL - plano-convex lens; PD - photodiode; PMT - photomultiplier tube.

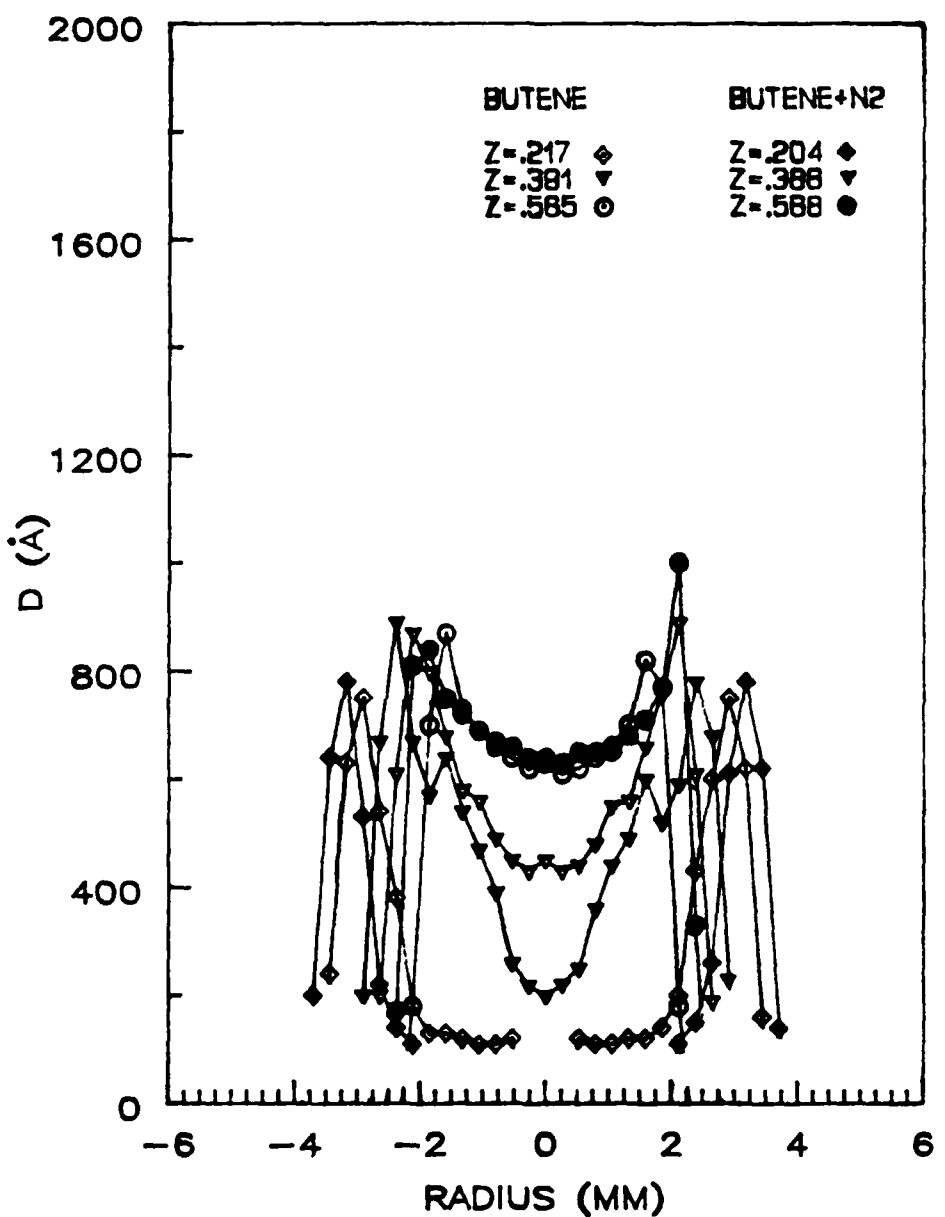


Figure A-3. Particle diameter as a function of radius and nondimensionalized height for the lower region of the butene flames.

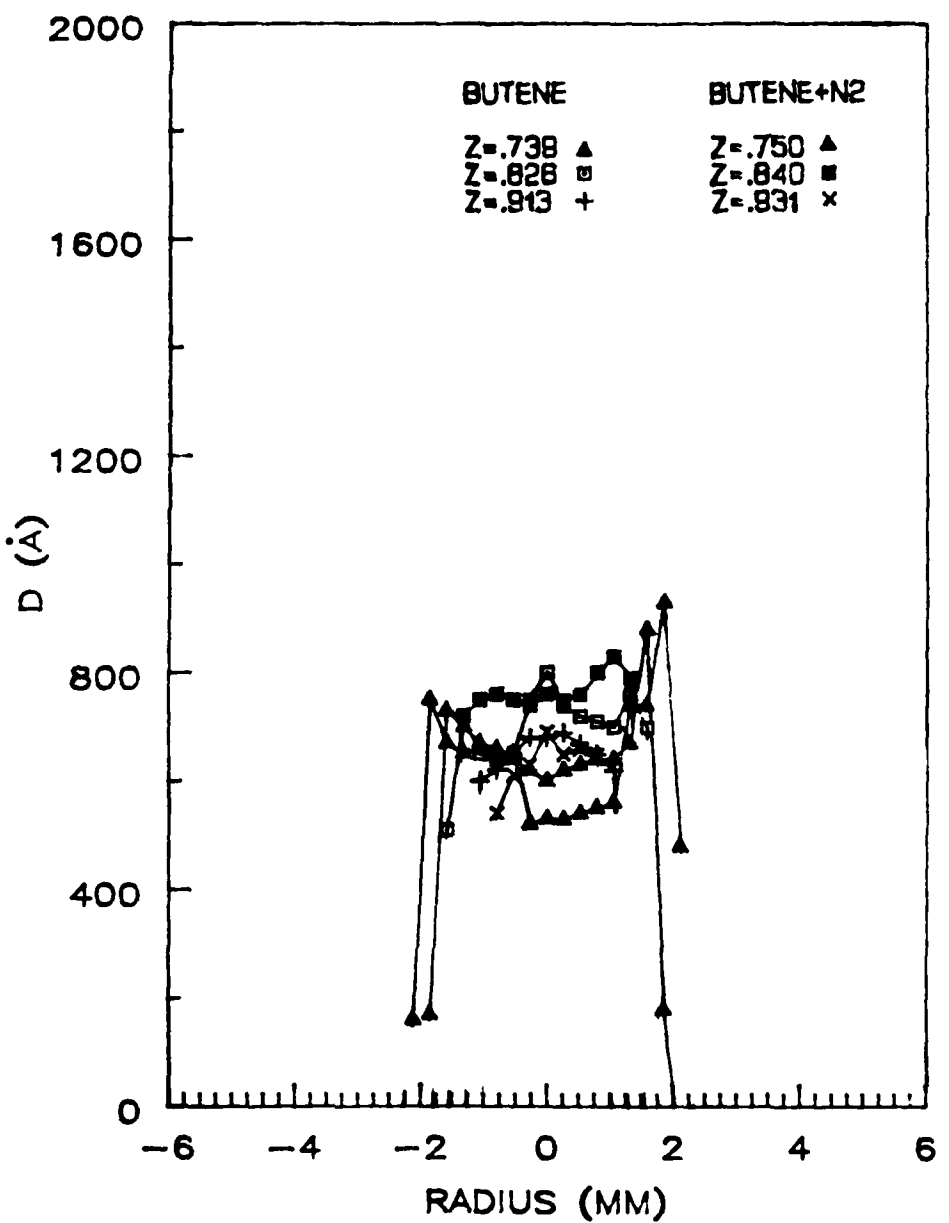


Figure A-4. Particle diameter as a function of radius and nondimensionalized height for the upper region of butene flames.

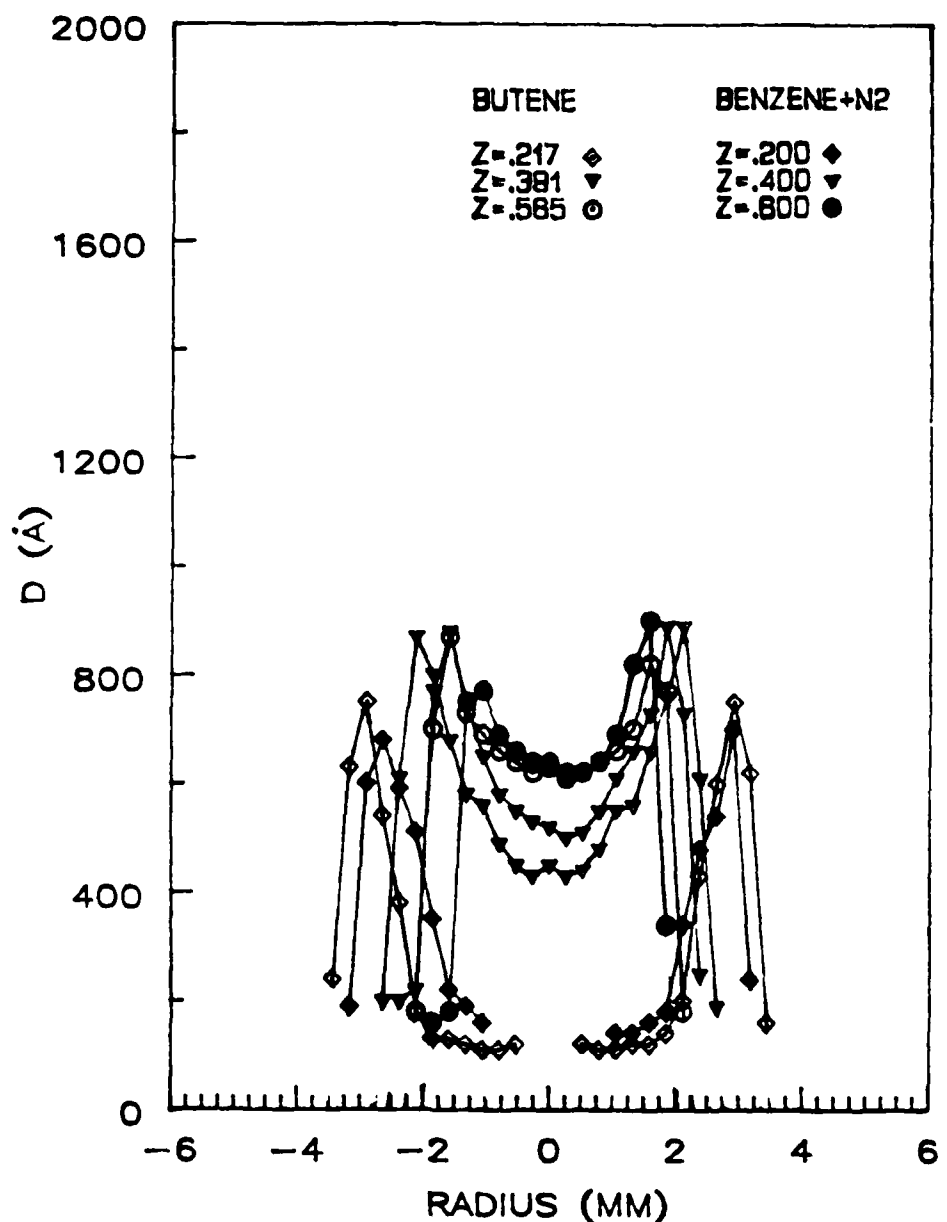


Figure A-5. Particle diameter as a function of radius and nondimensionalized height for the lower region of the undiluted butene flame and the diluted benzene flame.

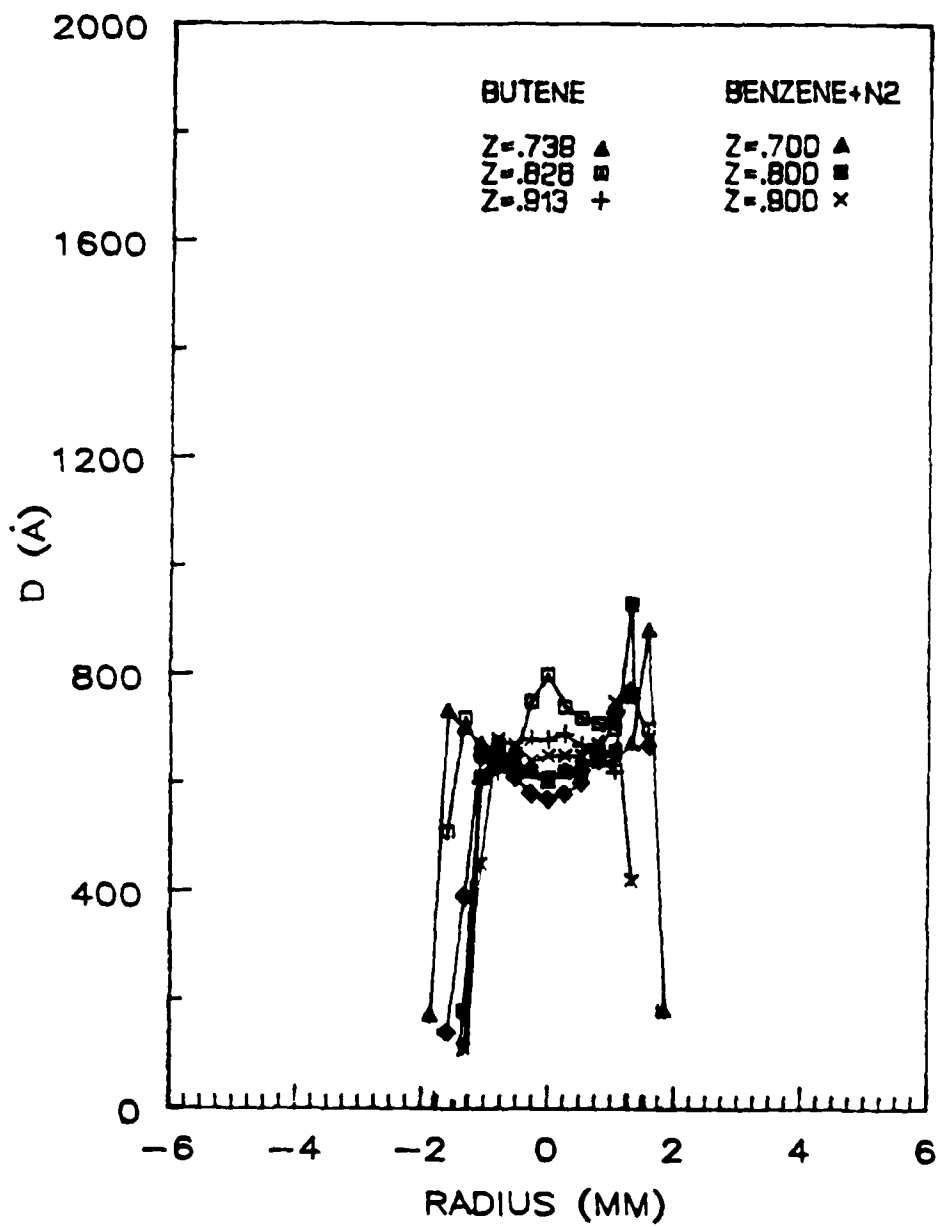


Figure A-6. Particle diameter as a function of radius and nondimensionalized height for the upper region of the undiluted butene flame and the diluted benzene flame.

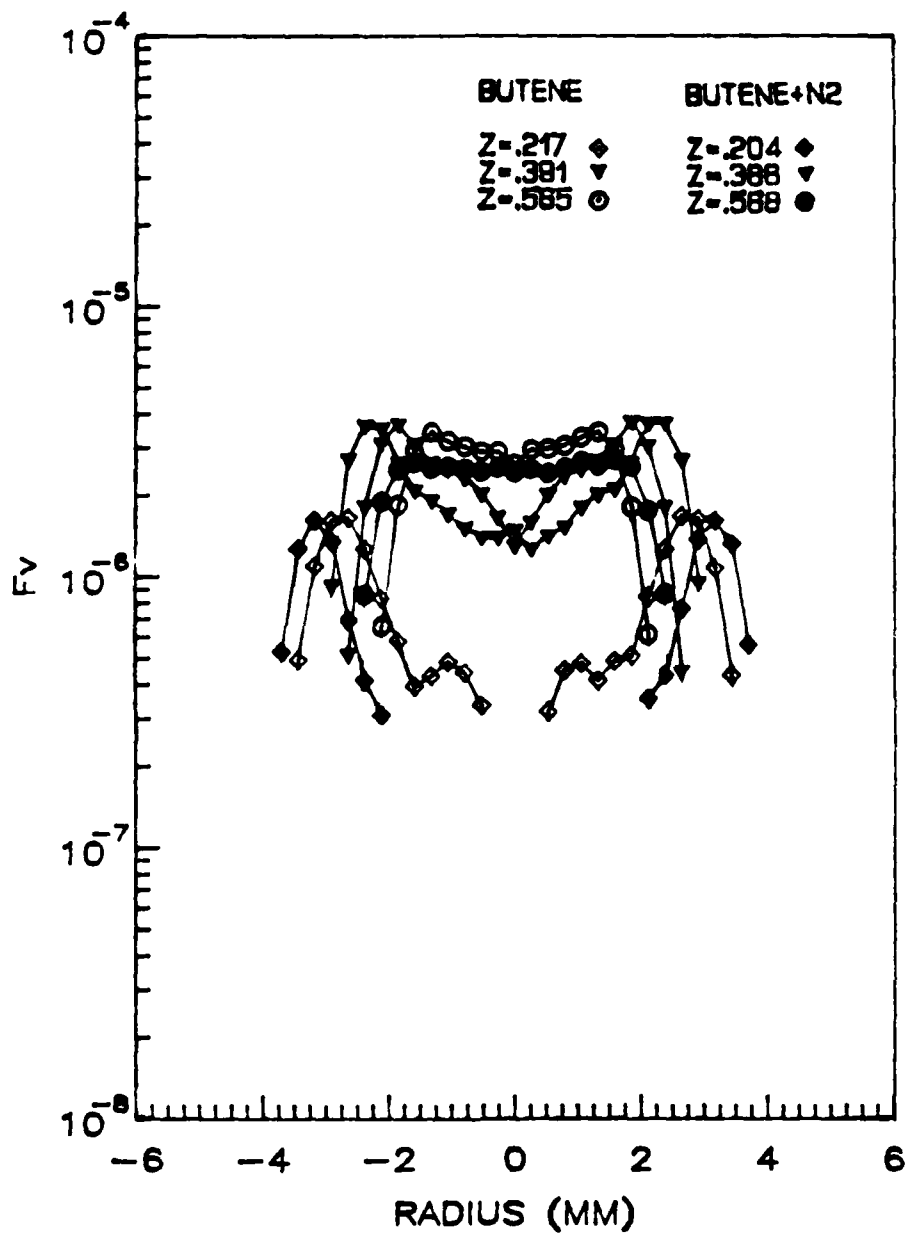


Figure A-7. Volume fraction or function of radius and nondimensionalized height for the lower region of the butene flames.

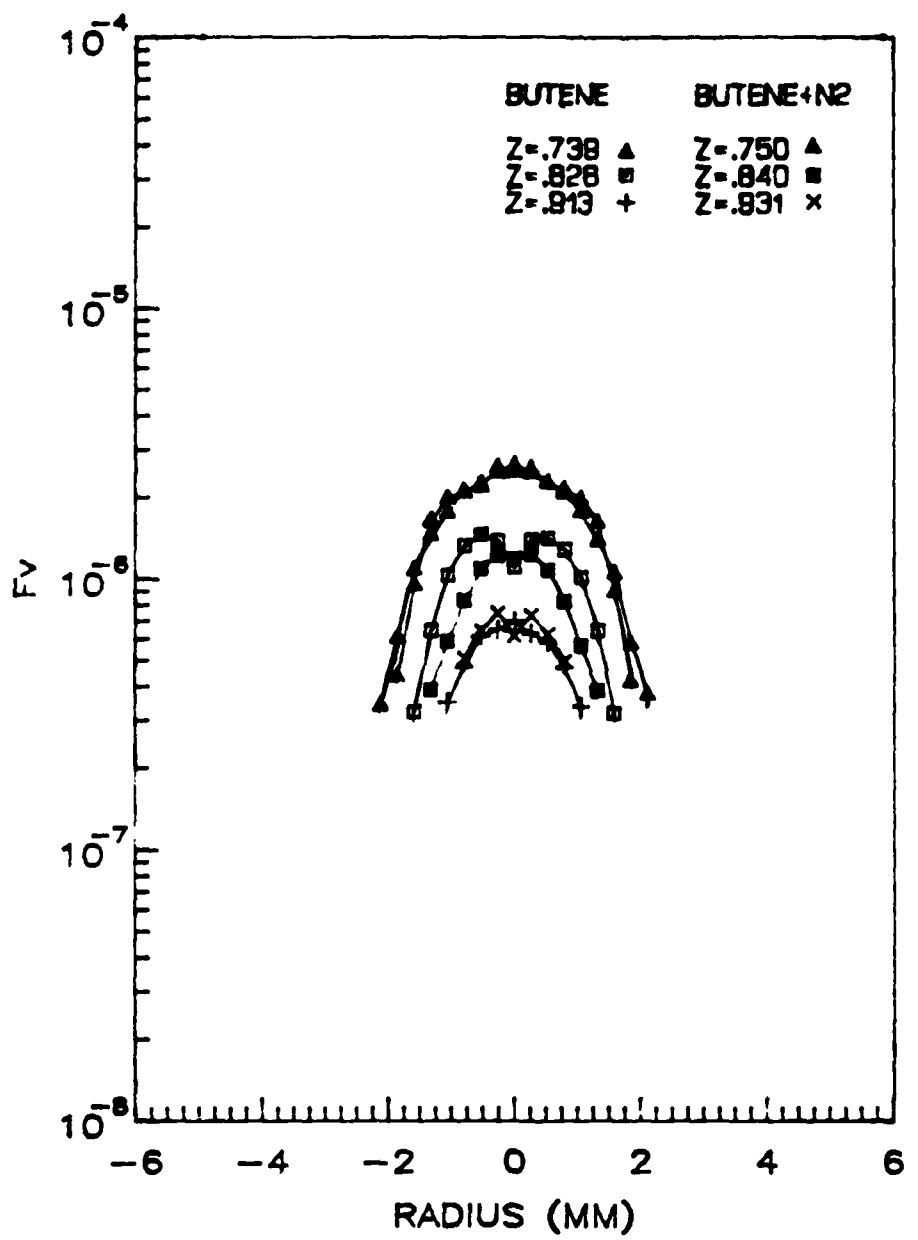


Figure A-8. Volume fraction as a function of radius and nondimensionalized height for the lower region of the butene flames.

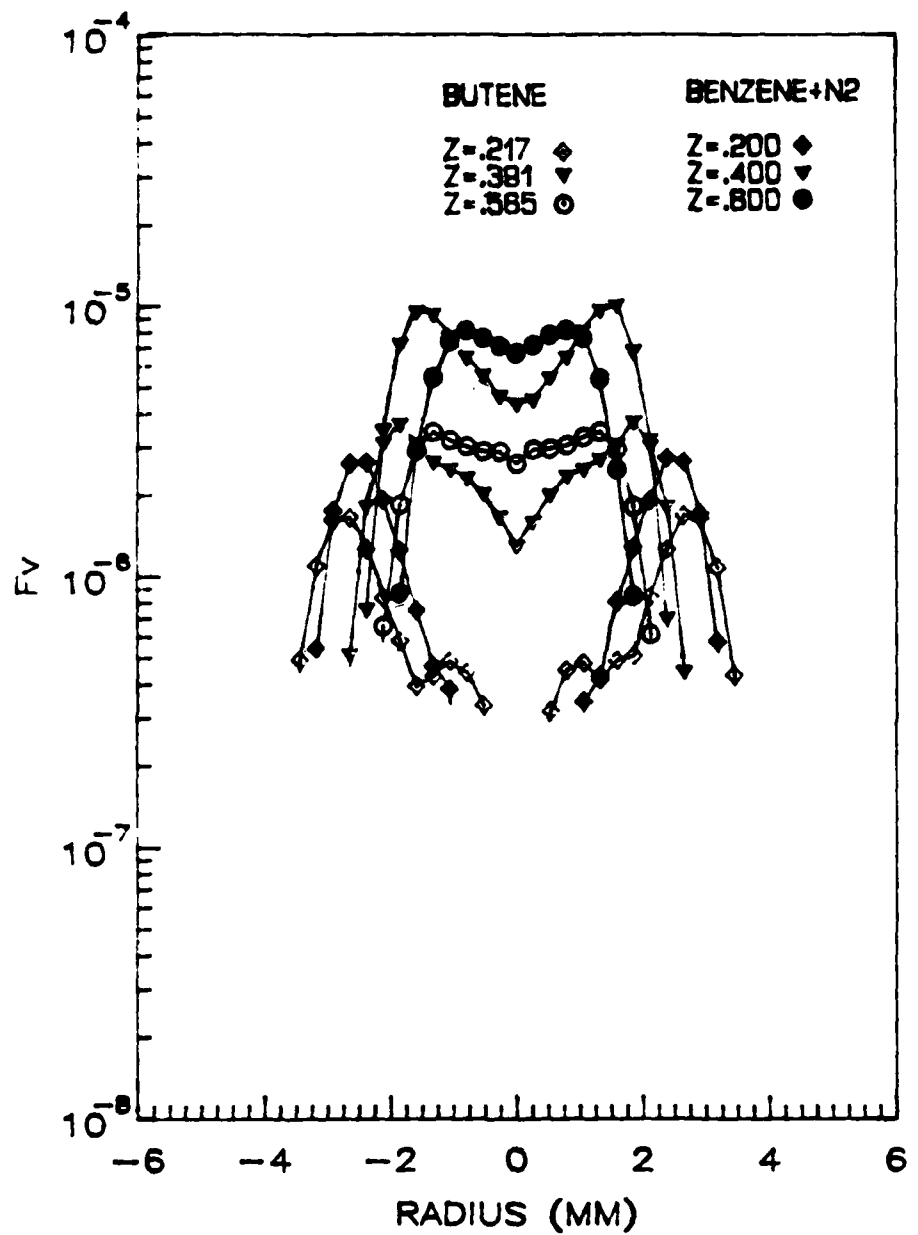


Figure A-9. Volume fraction as a function of radius and nondimensionalized height for the lower region of the undiluted butene flame and the diluted benzene flame.

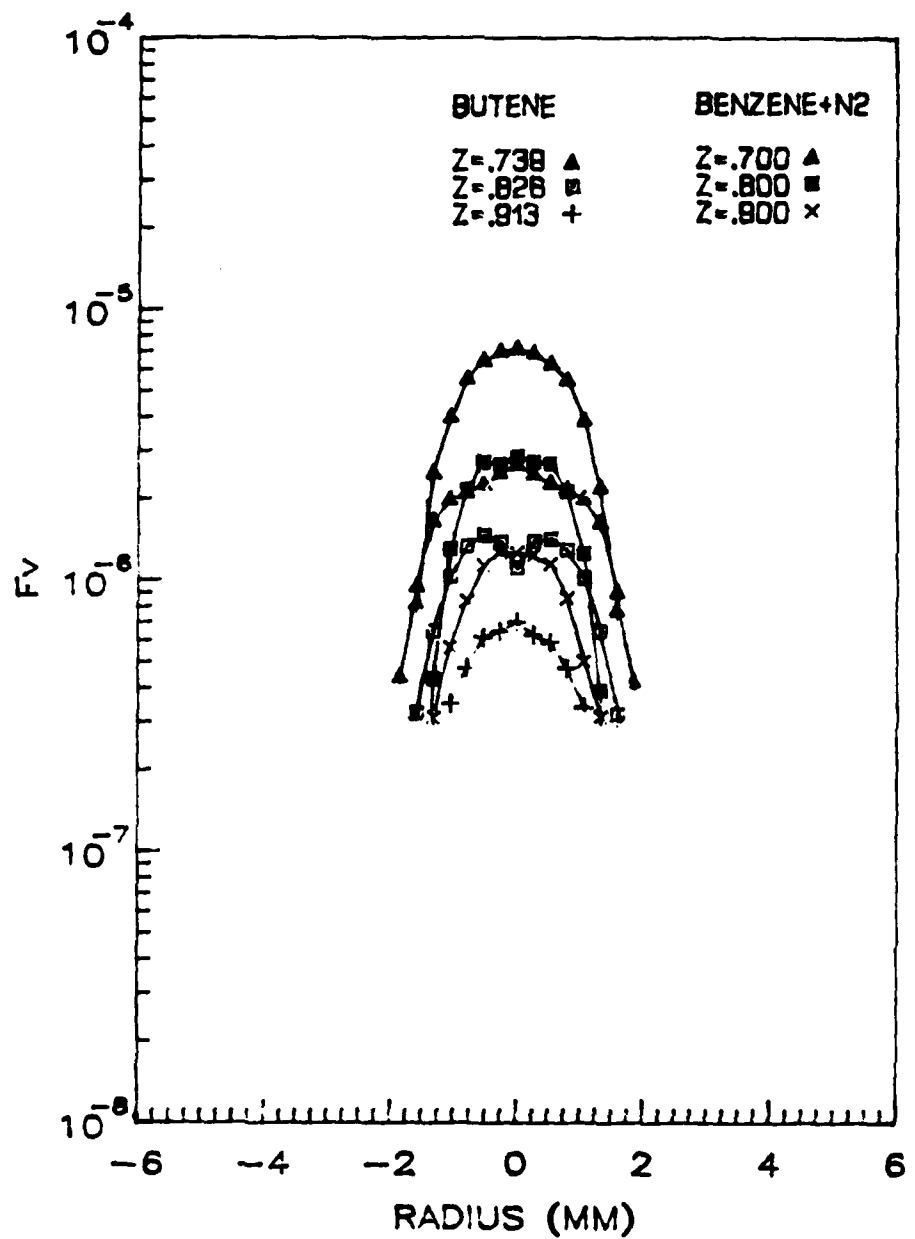


Figure A-10. Volume fraction as a function of radius and nondimensionalized height for the upper region of the undiluted butene flame and the diluted benzene flame.

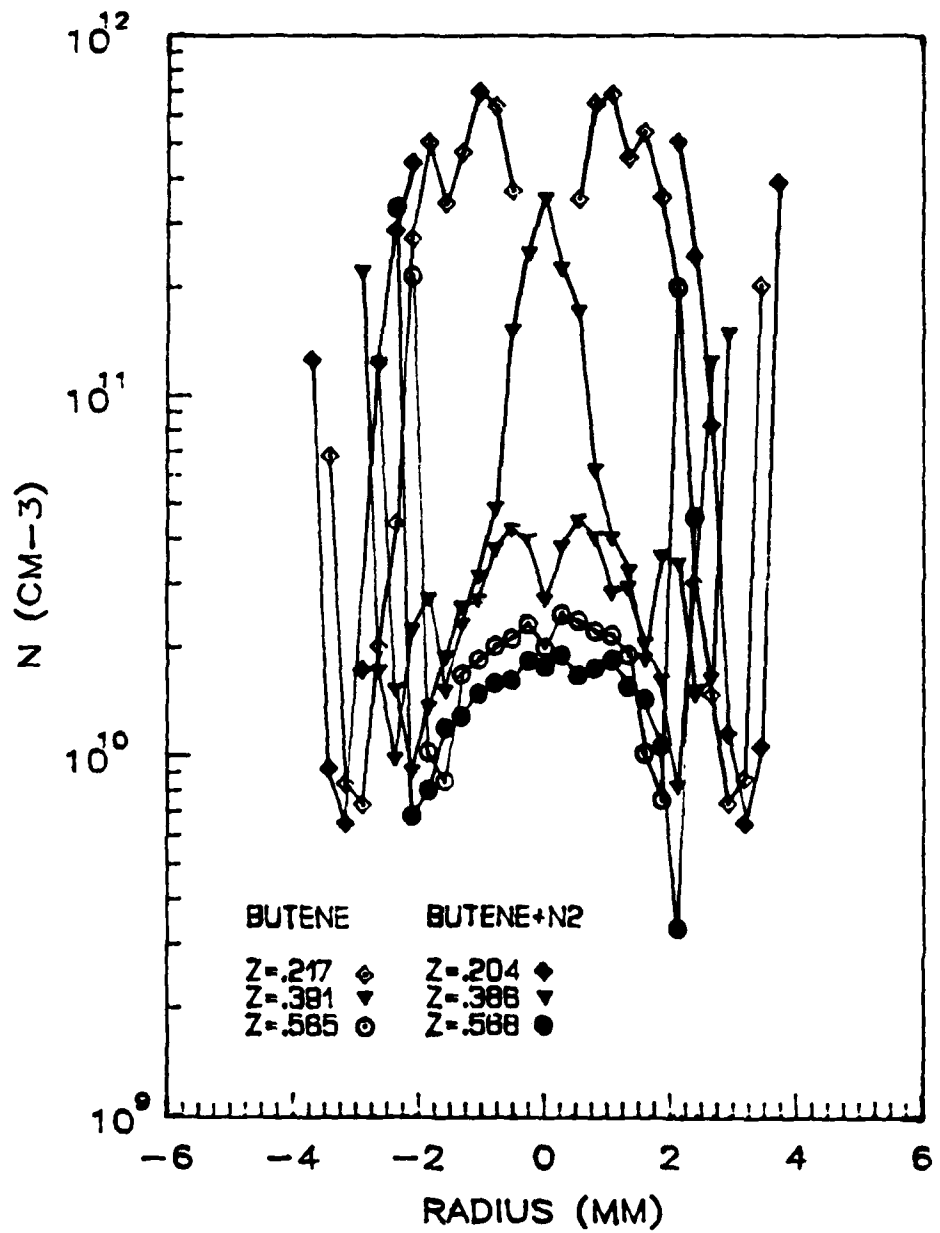


Figure A-11. Number density as a function of radius and nondimensionalized height for the lower region of the butene flames.

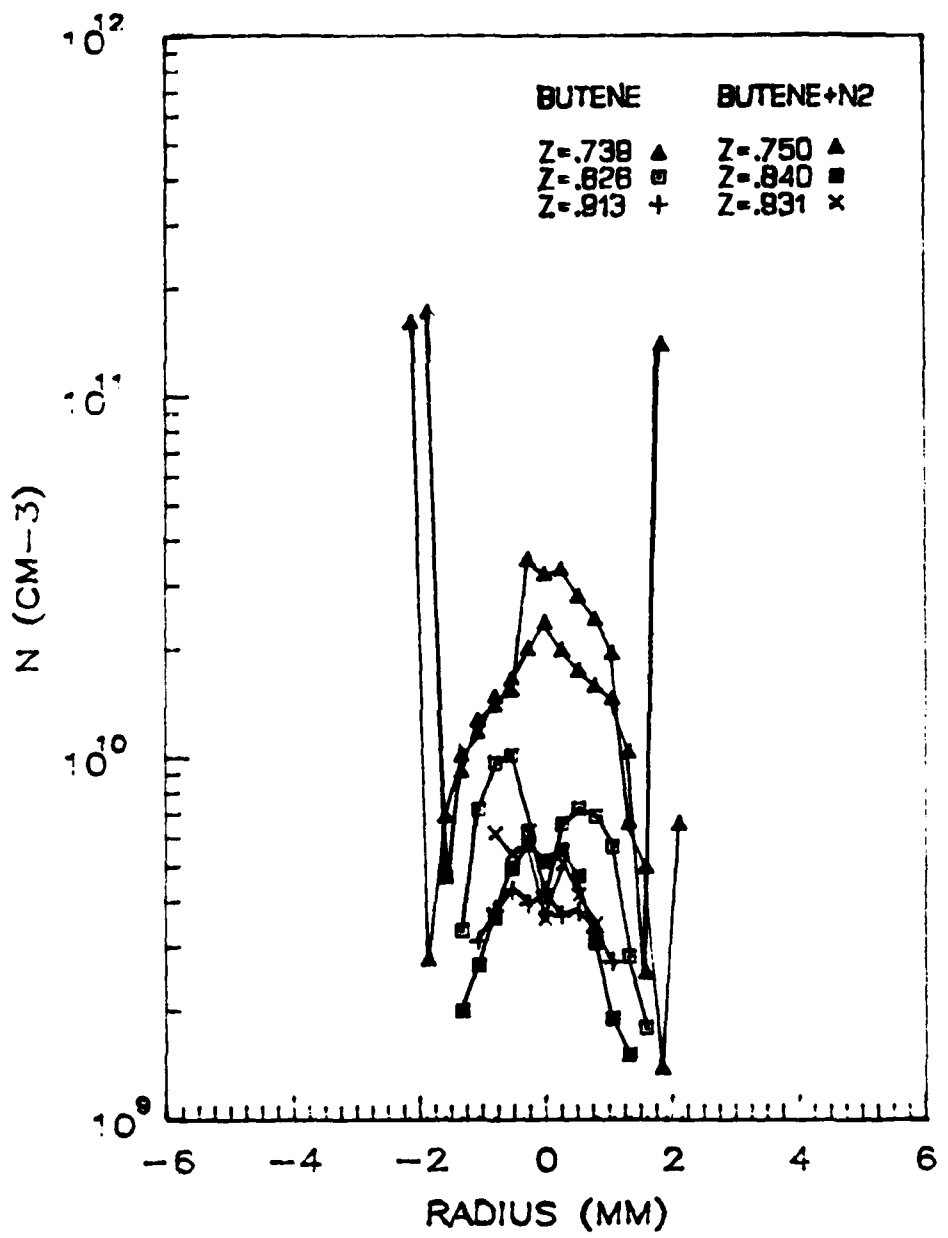


Figure A-12. Number density as a function of radius and nondimensionalized height for the upper region of butene flames.

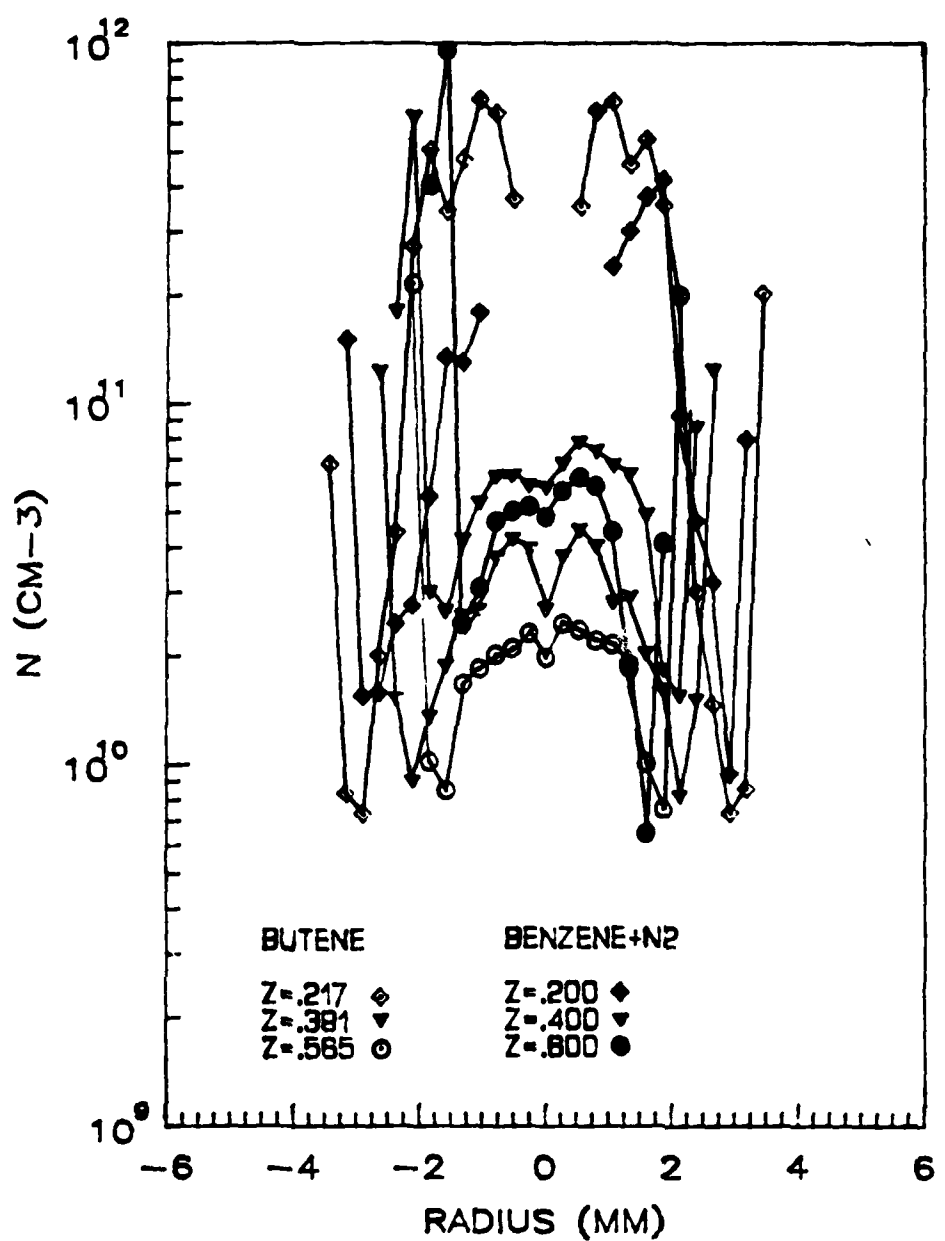


Figure A-13. Number density as a function of radius and nondimensionalized height for the lower region of the undiluted butene flame and the diluted benzene flame.

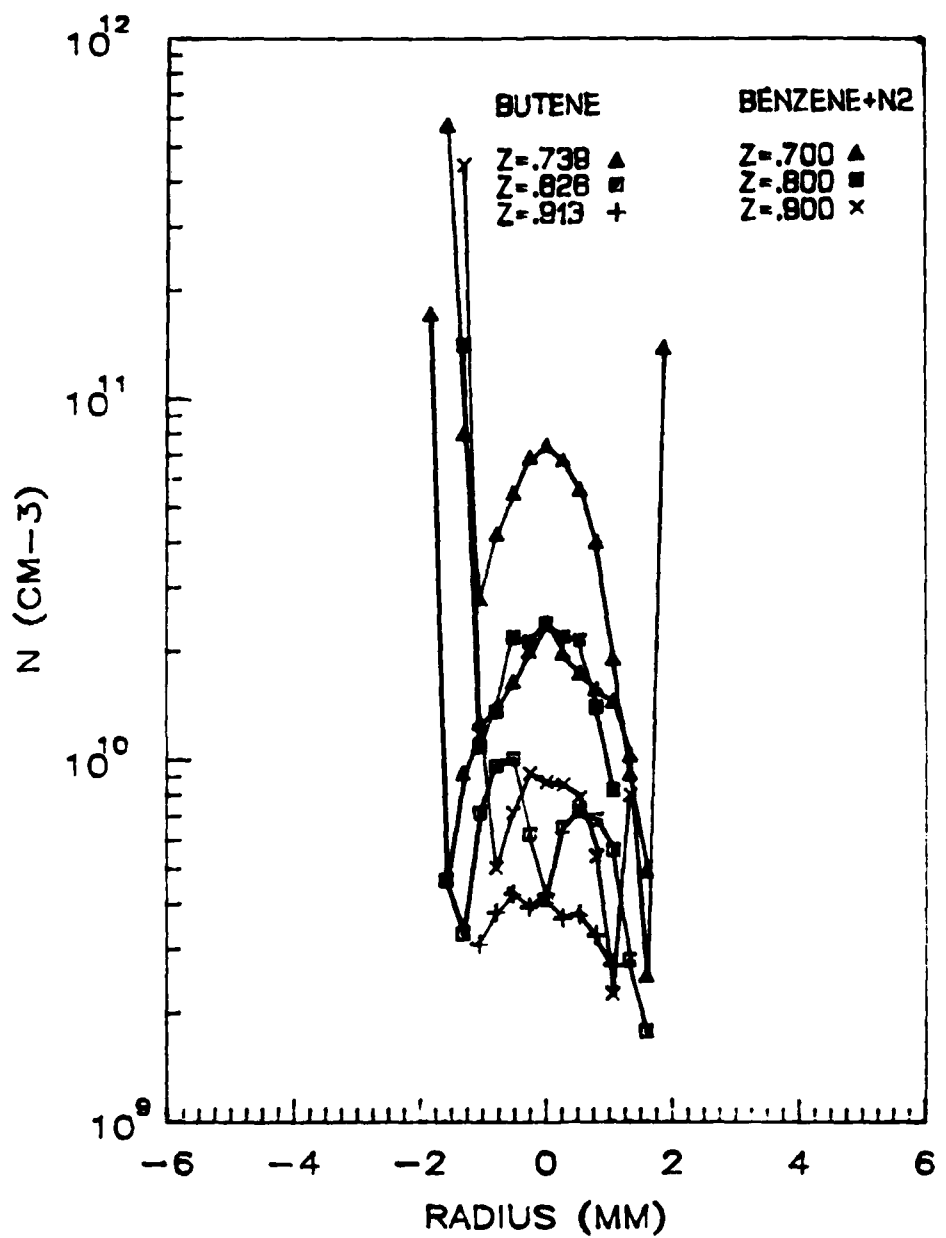


Figure A-14. Number density as a function of radius and nondimensionalized height for the upper region of the undiluted butene flame and the diluted benzene flame.

END

FILMED

3-85

DTIC